

5-15-2008

## Manufacturing Process Design and Control Based on Error Equivalence Methodology

Shaoqiang Chen  
*University of South Florida*

Follow this and additional works at: <https://digitalcommons.usf.edu/etd>



Part of the [American Studies Commons](#)

---

### Scholar Commons Citation

Chen, Shaoqiang, "Manufacturing Process Design and Control Based on Error Equivalence Methodology" (2008). *USF Tampa Graduate Theses and Dissertations*.  
<https://digitalcommons.usf.edu/etd/173>

This Thesis is brought to you for free and open access by the USF Graduate Theses and Dissertations at Digital Commons @ University of South Florida. It has been accepted for inclusion in USF Tampa Graduate Theses and Dissertations by an authorized administrator of Digital Commons @ University of South Florida. For more information, please contact [digitalcommons@usf.edu](mailto:digitalcommons@usf.edu).

Manufacturing Process Design and Control Based on Error Equivalence Methodology

by

Shaoqiang Chen

A thesis submitted in partial fulfillment of  
the requirements for the degree of  
Master of Science in Industrial Engineering  
Department of Industrial and Management Systems Engineering  
College of Engineering  
University of South Florida

Major Professor: Qiang Huang, Ph.D.  
Michael Weng, Ph.D.  
Susana Lai-Yuen, Ph.D.

Date of Approval:  
May 15, 2008

Keywords: variation reduction, statistical process control, engineering driven,  
equivalence mechanism, tolerance synthesis, diagnosis, root cause identification

© Copyright 2008, Shaoqiang Chen

Dedication

To My Parents

## Acknowledgements

I would like to express my gratitude to my major advisor Dr. Qiang Huang, whose expertise, understanding, and patience, added considerably to my graduate experiences. I appreciate his vast knowledge and skills in many areas.

I want to thank the other members of my committee, Dr. Michael Weng, and Dr. Susana Lai-Yuen, for the assistance they provided at all levels of the research project. I wish to thank Dr. José Zayas-Castro who provided me with the teaching assistantship. Sincerely gratitude is also given to all other faculty members who have taught me many important courses in USF. Special thanks should be given to Ms. Gloria Hanshaw and Ms. Jackie Stephens, who helped me with much required paperwork every semester.

A very sincere and warm-hearted gratitude goes to Hui Wang, who has provided all kinds of help to me during my study in USF. Without all of his help and his kind heart, I could not smoothly work out many problems in the USA.

In addition, I would like to express my sincere appreciation to Xi Zhang, Yang Tan, Qingwei Li, Diana Prieto, Patricio Rochia, Athina Brintaki, and other IMSE friends. I also thank Don McLawhorn, who helped me improve my English.

Finally, I am forever indebted to my parents Xiaojun Chen and Yulian Sun, for their endless love, without which I would not have finished this thesis.

## Table of Contents

List of Tables	iii
List of Figures	iv
Abstract	vi
Chapter 1 Introduction	1
1.1 Error Equivalence and Variation Equivalence Phenomena	3
1.2 Related Work and the State of the Arts	5
1.2.1 Literature Review for Process Modeling	6
1.2.2 Literature Review for Process Design and Optimization	8
1.2.3 Literature Review for Process Control: Root Cause Diagnosis	10
1.2.4 Summary of the Literature Review	13
1.3 Thesis Outline	14
Chapter 2 Error Equivalence Based Process Design and Optimization	16
2.1 The Error Equivalence Based Process Design and Optimization	17
2.1.1 Allocate Tolerance to Aggregated Error Sources at Each Manufacturing Stage	17
2.1.2 Error Equivalence Based Global Process Design Optimization	21
2.2 Case Study	25
2.2.1 Illustrate the Approach Using a Multistage Machining Process	25
2.2.2 Remark on Sensitivity Analysis of the Optimal Process Design	34
2.3 Chapter Summary	35
Chapter 3 Diagnose Multiple Variation Sources under Variation Equivalence	37
3.1 Concept of Variation Equivalence and Equivalent Variation Patterns Library	38
3.1.1 Definition of Variation Equivalence	38
3.1.2 Equivalent Covariance Structure Analysis and Library	39
3.2 Diagnosis and Root Cause Identification under Variation Equivalence	47
3.3 Case Study	51
3.3.1 Illustration of the Root Cause Diagnosis Approach Using a Machining Process	51

3.3.2 Remark on the Excitation-Response Path Approach	53
3.4 Chapter Summary	54
Chapter 4 Conclusions and Future Work	56
4.1 Conclusions	56
4.2 Future Work	57
Cited References	59
Appendices	66
Appendix A: Review of EFE and Derivation of $\Delta d$	67
Appendix B: Prediction and Estimation of Kriging Model	69
Appendix C: Derivation of the Equivalent Covariance Structures	70
About the Author	End Page

## List of Tables

Table 2.1	Design Variables Range under GCS (unit: mm)	32
-----------	---	----

## List of Figures

Figure 1.1	Error Equivalence in Machining Process	4
Figure 1.2	Error Equivalence in Assembly Process	4
Figure 2.1	Procedure of Error Equivalence Based Process Design and Optimization	17
Figure 2.2	Workpiece and Locating Scheme (Wang, <i>et al.</i> , 2005)	26
Figure 2.3	Operation Steps	26
Figure 3.1	A 2-D Machining Process Example of Variation Equivalence	39
Figure 3.2	Variation Equivalence of Faulty Condition 1	42
Figure 3.3	Variation Equivalence of Faulty Condition 2	43
Figure 3.4	Variation Equivalence of Faulty Condition 3	44
Figure 3.5	Variation Equivalence of Faulty Condition 4	44
Figure 3.6	Variation Equivalence of Faulty Condition 5	45
Figure 3.7	Variation Equivalence of Faulty Condition 6	46
Figure 3.8	Variation Equivalence of Faulty Condition 7	47
Figure 3.9a	Eigenvectors Gestures	51
Figure 3.9b	Sample Slope and Population Slope	51
Figure 3.10	Excitation-Response Path of Case Study Result	52

Figure 3.11	Excitation-Response Path Using Reference Vector $(1\ 0\ 0)^T$	53
Figure 3.12	Excitation-Response Path Using Reference Vector $(0\ 1\ 0)^T$	54

# Manufacturing Process Design and Control Based on Error Equivalence Methodology

Shaoqiang Chen

## ABSTRACT

Error equivalence concerns the mechanism whereby different error sources result in identical deviation and variation patterns on part features. This could have dual effects on process variation reduction: it significantly increases the complexity of root cause diagnosis in process control, and provides an opportunity to use one error source as based error to compensate the others.

There are fruitful research accomplishments on establishing error equivalence methodology, such as error equivalence modeling, and an error compensating error strategy. However, no work has been done on developing an efficient process design approach by investigating error equivalence. Furthermore, besides the process mean shift, process fault also manifests itself as variation increase. In this regard, studying variation equivalence may help to improve the root cause identification approach. This thesis presents engineering driven approaches for process design and control via embedding error equivalence mechanisms to achieve a better, insightful understanding and control of manufacturing processes.

The first issue to be studied is manufacturing process design and optimization based on the error equivalence. Using the error prediction model that transforms different types of errors to the equivalent amount of one base error, the research derives a novel process tolerance stackup model allowing tolerance synthesis to be conducted. Design of computer experiments is introduced to assist the process design optimization.

Secondly, diagnosis of multiple variation sources under error equivalence is conducted. This allows for exploration and study of the possible equivalent variation patterns among multiple error sources and the construction of the library of equivalent covariance matrices. Based on the equivalent variation patterns library, this thesis presents an excitation-response path orientation approach to improve the process variation sources identification under variation equivalence.

The results show that error equivalence mechanism can significantly reduce design space and release us from considerable symbol computation load, thus improve process design. Moreover, by studying the variation equivalence mechanism, we can improve the process diagnosis and root cause identification.

## Chapter 1

### Introduction

Variation reduction is of vital importance for manufacturing process and product quality improvement due to uncertainty in the processes. It has received considerable attention from the manufacturing community because of the intense global competition. There are two main categories of approaches for process variation reduction: data driven approaches such as statistical process control (SPC), and engineering driven approaches. SPC can detect process quality changes. However, it casts little light on engineering knowledge about the root cause, which needs efforts of engineers to figure out the sources of the quality changes. Engineering driven approaches fill this gap, and have significantly improved manufacturing processes variation reduction. However, there are still some process phenomena that have not been well addressed. One phenomenon named “error equivalence” concerns the mechanism whereby different error sources result in identical deviation and variation patterns on part features. This could have dual effects on process variation reduction: it significantly increases the complexity of root cause diagnosis in process control, and provides an opportunity to use one error source as based error to compensate the others.

Although there are fruitful research accomplishments on establishing error equivalence methodology, such as error equivalence modeling, and error compensating error strategy, variation reduction for the process design and control is still an extremely challenging issue for the following reasons:

- *Lack of an efficient process design approach under error equivalence.* For early process design stage, process tolerance strategy is crucial to control of product/process inaccuracy and imperfection. Previous tolerance synthesis has been carried out simultaneously in product design and process design. However, the traditional tolerance synthesis was conducted among different error sources. When the number of manufacturing stage increase, the dimension of design space will considerably increase. Thus, this fact impacts the efficiency of the early stage process design.
- *Lack of an efficient approach for process variation control under identical variation pattern from multiple error sources.* Although root cause identification draws significantly attention in recent years, there still exists a lack of consideration on the phenomenon that different error sources may result in the identical product feature variation pattern. Therefore, when there are multiple error sources in a manufacturing process, root cause identification of variation sources will be typically a challenge. Since the equivalent variation patterns could conceal the information of multiple errors and thus significantly increase the complexity of root cause identification (diagnosis). Meanwhile, this fact may provide an opportunity to purposely study the

part feature variation patterns of equivalent error sources and thus derive a more efficient variation sources identification approach.

Therefore, the aforementioned issues entail an essential analysis of error equivalence for process design and control improvement. The goal of this work is to utilize the error equivalence in manufacturing to achieve an insightful understanding of process variation for developing a better process design strategy and control approach.

### 1.1 Error Equivalence and Variation Equivalence Phenomena

In a manufacturing process, product quality can be affected by multiple error sources. For example, the dominant root cause of quality problems in a machining process includes fixture, datum, and machine tool errors. A fixture is a device used to locate, clamp, and support a workpiece during machining, assembly, or inspection. Fixture error is considered to be a significant fixture deviation of a locator from its specified position. Machining datum surfaces are those part features that are in direct contact with the fixture locators. Datum error is deemed to be the significant deviation of datum surfaces and is mainly induced by imperfections in raw workpieces or faulty operations in the previous stages. Together the fixture and datum surfaces provide a reference system for accurate cutting operations using machine tools. Machine tool error is modeled in terms of significant tool path deviations from its intended route. This thesis mainly focuses on kinematics aspects of these three error types.

A widely observed engineering phenomenon is that different individual error sources can result in the identical deviation and variation patterns on product features in manufacturing process. For instance, in a machining process, all aforementioned process deviations can generate the same amount of feature deviation  $x$  as shown in Fig. 1.1 (Wang, Huang, and Katz, 2005; and Wang and Huang, 2006). This error equivalence phenomenon is also observed in many other manufacturing processes, e.g., the automotive body assembly process (Fig. 1.2, Ding, *et al.*, 2005).

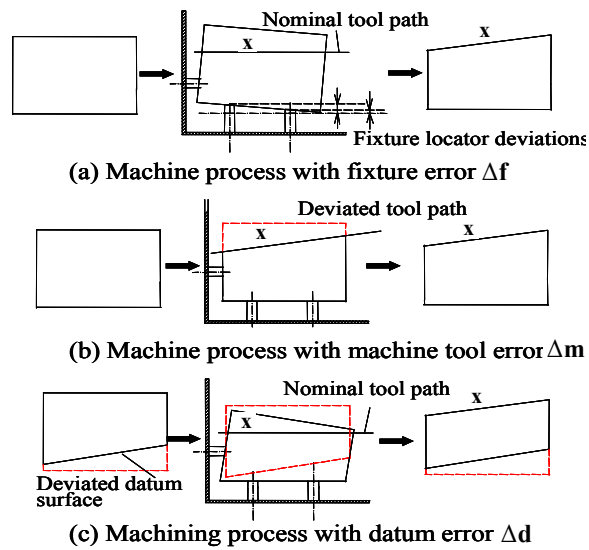


Figure 1.1 Error Equivalence in Machining Process

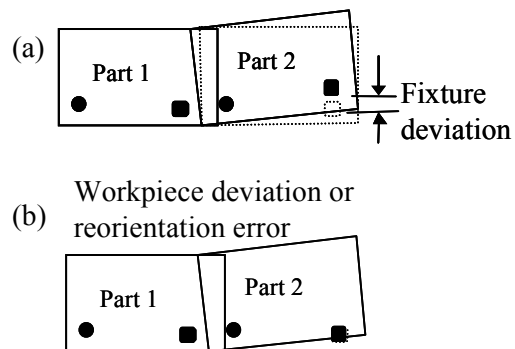


Figure 1.2 Error Equivalence in Assembly Process

The impact of such an error equivalence phenomenon on manufacturing process control is twofold. On the one hand, it significantly increases the complexity of variation control. As an example, identifying the root causes becomes extremely challenging when different error sources are able to produce the identical dimensional variations. On the other hand, the error equivalence phenomenon provides an opportunity to purposely use one error source as base error in the early stage of process design, thus efficiently improving the tolerance strategy for the manufacturing process.

In both cases, a fundamental understanding of this complex engineering phenomenon will assist to improve manufacturing process design and control.

## 1.2 Related Work and the State of the Arts

Before 2005, the study on error equivalence is very limited. Most related research on process error modeling has been focused on the analysis of individual error sources, e.g., the fixture errors and/or machine tool errors, how these errors impact the product quality, and thereby how to diagnose the errors and conduct feedback adjustment to reduce variation. Since Wang *et al.*, 2005, there have been some studies on the error equivalence for the above issues. This Section reviews the related research on process modeling, process design and optimization, and process root cause diagnosis.

### 1.2.1 Literature Review for Process Modeling

In this Section, we will review error equivalence modeling and process modeling. For error equivalence modeling, Wang *et al.*, 2005, utilized the error equivalence phenomena to develop the error equivalence modeling. In the error equivalence model, different error sources (e.g., fixture error, machine tool error and datum error) were linearly transformed into one based error, i.e., equivalent fixture error (EFE). After transforming the different types of error into one based error, we can aggregate the equivalent errors. This will be of great benefit to the process error prediction and variation propagation modeling, since it will significantly reduce the dimension of input variables, which will be introduced in detail in Section 2.1.1 of Chapter 2. The error equivalence mechanism also helped to understand the process error compensating error strategy. Wang and Huang, 2006, used the equivalent fixture error modeling in error cancellation and applied it in machining process control and deviation feedback adjustment.

The process modeling in the literature is summarized as causality modeling. Models of predicting surface quality are often deterministic and used for a single machining station (Li and Shin, 2006). In the recent decade, more research can be found to investigate the causal relationship between part features and errors, especially in a complex manufacturing system. The available model formulation includes time series model (Lawless, Mackay, and Robinson, 1999), state space models (Jin and Shi, 1999; Ding, Ceglarek, and Shi, 2000; Huang, Shi, and Yuan, 2003; Djurdjanovic and Ni, 2001;

Zhou, Huang, and Shi, 2003; and Huang and Shi, 2004), and state transition model (Mantripragada and Whitney, 1999). The results of the process error model can be summarized as follows. Denote by  $\mathbf{x}$  the dimensional deviation of a workpiece of  $N$  operations and by  $\mathbf{u} = (u_1, u_2, \dots, u_p)^T$  the multiple error sources from all operations. The relationship between  $\mathbf{x}$  and  $\mathbf{u}$  can be represented by

$$\mathbf{x} = \sum_{i=1}^p \Gamma_i \mathbf{u}_i + \boldsymbol{\varepsilon} = \mathbf{\Gamma} \mathbf{u} + \boldsymbol{\varepsilon}, \quad (1.1)$$

where  $\Gamma_i$ 's are sensitivity matrices determined by process and product design and  $\mathbf{\Gamma} = [\Gamma_1 \mid \Gamma_2 \mid \dots \mid \Gamma_p]$ .  $\boldsymbol{\varepsilon}$  is the noise term. This line of research (Hu, 1997; Jin and Shi, 1999; Mantripragada and Whitney, 1999; Djurdjanovic and Ni, 2001; Camelio, Hu, and Ceglarek, 2003; Agapiou, *et al.*, 2003; Agapiou, *et al.*, 2005; Zhou, *et al.*, 2003; Huang, Zhou, and Shi, 2002; Zhou, Huang, and Shi, 2003; Huang, Shi, and Yuan, 2003; and Huang and Shi, 2004) provides a solid foundation for conducting further analysis of the error equivalence.

Based on the aforementioned research on process modeling, Wang *et al.*, 2005, developed a multi-operational machining processes variation propagation model for sequential root cause identification and measurement reduction by imbedding the error equivalence mechanism, which helped to better understand and model the mechanism that different error sources result in the identical variation pattern on part features. The derived quality prediction model (causal model) embedded with error equivalence mechanism can reveal more physical insights into the process variation.

Summarizing the research on process error prediction and variation propagation modeling, we can see that causality modeling well connect the process errors and product feature quality. Moreover, integrating error equivalence into causality modeling can be a considerable benefit. Because introducing error equivalence to process modeling helps to shrink the dimension of input variables. The reduction design space is of great importance to early stage process design efficiency.

### 1.2.2 Literature Review for Process Design and Optimization

Design of a multistage machining process involves tolerance allocation at each stage and design of process layouts, in particular, the fixture layouts. Tolerancing strategy is therefore crucial to control of product/process inaccuracy and imperfection. Conventional tolerance synthesis has been carried out simultaneously in product design and process design. A major goal of tolerance synthesis at design stage is to reduce quality loss (Taguchi, 1989; Choi *et al.*, 2000; and Pramanik *et al.*, 2005), while tolerance synthesis for process design aims at manufacturing cost reduction. As an example, tolerance charting (Wade, 1967; Ngoi and Ong, 1993, 1999; and Xue and Ji, 2005) converted the designed tolerances of products to manufacturing tolerances. Optimal tolerance allocation for process selection has also been widely studied (Nagarwala *et al.*, 1994; Singh *et al.*, 2004; and Wang and Liang, 2005). Recent research (Shiu *et al.*, 2003; and Dong *et al.*, 2005) considered deformations in manufacturing processes as well.

Simultaneous tolerance synthesis considers both design and manufacturing tolerances and has attracted more attentions in the past decade. Zhang *et al.*, 1992, conducted optimization of design and tolerance allocation to select processes among alternatives. An analytical model (Zhang and Wang, 2003) was also reported to simultaneously allocate design and machining tolerances based on a criterion of minimum manufacturing cost. Zhang, 1997, further established tolerance stackup model for assembly process. Recent research (Ye and Salustri, 2003; and Wang and Liang, 2005) on simultaneous tolerance synthesis incorporated both manufacturing cost and quality loss into the optimization function. Reviews of tolerancing research are available in Bjørke, 1989, Chase and Greenwood, 1988, Jeang, 1994, Royal *et al.*, 1991, Voelcker, 1998, Ngoi and Ong, 1998, and Hong and Chang, 2002.

Simultaneous tolerance synthesis is more challenging for a multistage manufacturing process. A commonly adopted approach is to model the impact of process parameters on tolerance stackup (Mantripragada and Whitney, 1999; Jin and Shi, 1999; Zhou *et al.*, 2003; and Huang *et al.*, 2003). Ding *et al.*, 2005, concurrently allocated component tolerances and selected fixtures for assembly processes using a state space model. Huang and Shi, 2003, conducted a study on simultaneous tolerance synthesis and optimal process selection for multistage machining processes.

Simultaneous tolerance synthesis, however, might generate a large design space. For example, in a milling or drilling process where parts are fixed under 3-2-1 locating scheme, the process variables involve tolerances of six fixture locators or six process

variables, machine tool paths (rotation and translation with six degrees of freedom), and datum surfaces. Thus, a multistage process will incur a large design space and makes it difficult to choose optimal and unique process design. One strategy is to prioritize the allocation of tolerances to different error sources at each stage through “proper” selection of cost functions. Since the cost function selection can be very subjective, especially when designing a new process where knowledge of cost structures is very limited, minor changes in cost functions could lead to dramatic changes in process design and tolerance allocation.

### 1.2.3 Literature Review for Process Control: Root Cause Diagnosis

Process control technology, which focuses on the detection, identification, diagnosis, and elimination of process faults, can help to reduce process downtime, and hence, the operation costs. The rapid advances in sensing and information technology that are currently being made mean that a large amount of data is readily available that requires process control methodologies to be developed for its interpretation. Statistical process control (SPC) (Montgomery, 2005, and the references therein) is the primary tool used in practice to improve the quality of manufacturing process. Although SPC can efficiently detect a departure from normal condition, it is unable to pin down the process fault that caused the alarm (root cause). And it is purely statistical data driven approach that inefficiently gives the process fault physical explanations. Therefore, the job of root cause identification is actually left to plant operators or quality engineers. In light of this

limitation of SPC, considerable research efforts have been expended on developing the approaches for root cause identification. Since process faults often manifest themselves as the shift of the mean values and the increase of variances, the root cause identification for process diagnosis can be categorized into two types: root cause identification of mean shift and of variation sources. The approaches developed for root cause diagnosis of variation sources include variation pattern mapping (Ceglarek and Shi, 1996, Jin and Zhou, 2006b, Li, *et al.*, 2007), variation estimation based on physical models (Apley and Shi, 1998; Chang and Gossard, 1998; Ding, Ceglarek, and Shi, 2002; Zhou, *et al.*, 2003; Camelio and Hu, 2004; Carlson and Söderberg, 2003; Huang, Zhou, and Shi, 2002; Huang and Shi, 2004; and Li and Zhou, 2006), and variation pattern extraction from measurement data (Jin and Zhou, 2006a).

Ceglarek, Shi, and Wu, 1994, developed root cause diagnostic algorithm for autobody assembly line where fixture errors are dominant process faults. Principal component analysis (PCA) has been applied to fixture error diagnosis by Hu and Wu, 1992, who make a physical interpretation of the principal components and thereby get insightful understanding of root causes of process variation. Ceglarek and Shi, 1996, integrated PCA, fixture design, and pattern recognition and have achieved considerable success in identifying problems resulting from worn, loose, or broken fixture elements in the assembly process. However, this method cannot detect multiple fixture errors. A PCA based diagnostic algorithm has also been proposed by Rong, Ceglarek, and Shi, 2000. Apley and Shi, 1998, developed a diagnostic algorithm that is able to detect multiple

fixture faults occurring simultaneously. Their continuing work in 2001 presented a factor analysis (Johnson, and Wichern, 1998) approach to diagnose root causes of process variability by using a causality model. Ding, Ceglarek, and Shi, 2002, derived a PCA based diagnostics from the state space model.

However, the number of the simultaneous error patterns may grow significantly as more manufacturing operations are involved. The multiple error patterns are rarely orthogonal and they are difficult to distinguish from each other. Therefore, the manufacturing process may not be diagnosable. Ding, Shi, and Ceglarek, 2002, analyzed the diagnosability of multistage manufacturing processes and applied the results to the evaluation of sensor distribution strategy. Variation component analysis (Rao, 1972, Rao and Kleffe, 1988) and mixed models (McCullagh, and Nelder, 1989, Pinheiro, and Bates, 2000) are also helpful to the diagnosability and diagnosis study. By using variance component analysis, Zhou, *et al.*, 2003, developed a more general framework for diagnosability analysis by considering aliasing faulty structures for coupled errors in a partially diagnosable process. Based on state space model and linear mixed effects model, Zhou *et al.*, 2004 developed a root cause estimation approach for manufacturing process. Further studies and research on root cause identification of multiple error sources have been achieved by Wang and Huang, 2006, utilizing the error equivalence concept and error cancellation modeling.

We can see that methods for diagnosis of different/equivalent patterns of single error/variation sources and different patterns of error/variation sources have been

developed. However, for the situation in which identical variation patterns happen, efforts are still needed for an efficient method. Because in a manufacturing process, an identical product feature variation pattern from multiple error sources can possibly occur.

#### 1.2.4 Summary of the Literature Review

The related research work in the literature is summarized as follows:

- *Process error prediction and variation propagation modeling.* Previous research work has been done on causality modeling with analysis of individual errors as well as equivalent errors in manufacturing processes. Also, the error equivalence based process modeling has assisted in understanding the error cancellation modeling and its application in process error root cause diagnosis and compensation. However, there is still large room for using the physical model that described the error equivalence to help understand some other issues, such as early stage process design and process variation sources identification.
- *Process design and optimization.* Traditional research on process tolerance design and optimization has extensively conducted the tolerance synthesis among different individual process errors. The optimization for design of process layout is also focusing on individual error sources. The design space and computation load will significantly increase as the number of manufacturing operation stages and process error sources increase. Therefore, previous research did not address a solution for an efficient method for the early stage process design.

- *Root cause diagnosis for process control.* Researchers have developed many methodologies of root cause identification for multistage manufacturing process diagnosis. These researches have involved in fault diagnosis for different variation patterns from single error sources, different variation patterns from different error sources. But no research work has been done on root cause identification for identical variation pattern from different error source, i.e., variation equivalence, while this phenomenon is an important engineering issue in manufacturing process.

### 1.3 Thesis Outline

In order to achieve an insightful understanding of manufacturing process variation and improve process quality, this thesis addresses the advances in: manufacturing process design and optimization strategy based on error equivalence methodology, and error equivalence analysis for root cause diagnosis of process variation. The following Chapters of this thesis are thus organized as follows:

Chapter 2 presents the modeling of process variation propagation and tolerance stackup model based on error equivalence. It utilizes the error equivalence mechanism to develop an efficient tolerance synthesis method for early process design stage. In addition, a globally process layout optimization model is developed for searching the optimal tolerance allocation among all the possible process design alternatives.

Chapter 3 studies the possible variation equivalence cases in a machining process and builds the equivalent variation patterns library. For process diagnosis, this Chapter

develops a new approach for root cause identification for identical variation pattern under multiple error sources.

Chapter 4 concludes the thesis. We also point out prospects of future research in this Chapter.

## Chapter 2

### Error Equivalence Based Process Design and Optimization

This Chapter aims to improve the simultaneous process tolerance synthesis for multistage manufacturing process by incorporating an error equivalence mechanism (Wang, Huang, and Katz, 2005; Wang and Huang, 2006) into tolerance stackup modeling and tolerance design. We propose to reduce design space by transforming multiple error sources into equivalent amount of “base” errors. The reduction of design space will assist to achieve a unique solution and global optimization of process design. Furthermore, we also embed error equivalence with computer experiments method to reduce the computation load for searching optimal process design.

The Chapter is organized as follows. Section 2.1 introduces the methodology of error equivalence based tolerance synthesis and optimal process design over the allowable design region. In Section 2.2, we illustrate the methodology through a case study of multistage machining process. To evaluate the robustness of the optimal process design, Section 3 also conducts sensitivity analysis. Conclusions are given in Section 2.3.

## 2.1 The Error Equivalence Based Process Design and Optimization

The proposed method consists of the following procedure illustrated by Fig. 2.1. First, we will generate a set of process layouts (design variables)  $\mathbf{s}_i$ 's through space filling design. For a given process layout  $\mathbf{s}_i$ , tolerance will be allocated to aggregated error sources (process variables) at each manufacturing stage (discussed in Section 2.1.1). The final tolerance stackup for all design variables  $\mathbf{s}_i$ 's will be used as responses in a Kriging model to identify the optimal fixture layout (presented in Section 2.1.2).

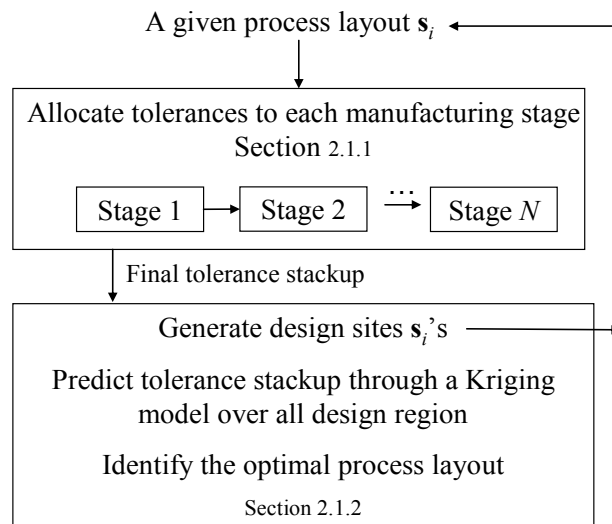


Figure 2.1 Procedure of Error Equivalence Based Process Design and Optimization

### 2.1.1 Allocate Tolerance to Aggregated Error Sources at Each Manufacturing Stage

Tolerance synthesis requires a thorough understanding on how the process variables impact the tolerance stackup. Therefore, the error equivalence based tolerance synthesis consists of tolerance stackup modeling and model based simultaneous tolerance allocation. We first present error equivalence based tolerance stackup modeling.

Tolerance stackup is mainly due to variation sources in each stage of a manufacturing process, e.g., machine tool error, datum error, and fixture error in a machining process. The objective of tolerance stackup modeling is to relate the stackup of tolerance in product features to all variation sources in a multistage manufacturing process. Existing tolerance stackup models roughly fall into three categories (Huang and Shi, 2003), namely, worst case model, root sum square model or interpolation of these two models, Monte Carlo simulation models, and physical models that study the impact of process variables on tolerance stackup. The tolerance stackup models in the third category provide a new opportunity of simultaneously allocating product and process tolerances (Ding *et al.*, 2005; and Huang and Shi, 2003). As discussed in Introduction, this approach unfortunately could generate a large design space as the number of processing stages increases.

We aim to reduce the design space and improve the tolerance stackup models in the third category. The main idea is to explore the relationship among multiple error sources, in particular, the error equivalence. Two types of error sources are called equivalent if they result in identical dimensional deviation. Equivalent error sources at each manufacturing stage therefore could be aggregated together when predicting feature deviations. In more detail, multiple types of errors  $\mathbf{x}_i$ 's can be transformed into a common base error through transformation  $\mathbf{x}_i^* = \mathbf{K}_i \mathbf{x}_i$ ,  $i=1,2,\dots,m$  (please refer to Appendix A for transformation matrices  $\mathbf{K}_i$ 's). Since fixture error is easier to be controlled and monitored, we choose fixture error to be the base error in this paper and transform all the error

sources into equivalent amount of fixture error (EFE). The product dimensional deviation can thus be predicted through the following model (Wang, Huang, and Katz, 2005):

$$\mathbf{y}_j(k) = \mathbf{\Gamma}_j \mathbf{u}(k) + \boldsymbol{\varepsilon}(k), \quad (2.1)$$

where  $\mathbf{y}_j(k)$  describes the feature deviations caused by aggregated error sources  $\mathbf{u}(k) = \sum_i \mathbf{x}_i^*(k)$  and process noise  $\boldsymbol{\varepsilon}(k)$  at the  $k$ th stage. Note that in traditional error

prediction model, the right hand side of Eqn. (2.1) contains not just one aggregated equivalence error vector in each stage, but a high dimensional vector that consists of different individual error sources, (e.g.,  $\mathbf{y}_j(k) = \mathbf{\Gamma}_j [\mathbf{x}_1(k) | \mathbf{x}_2(k) | \mathbf{x}_3(k)]^T + \boldsymbol{\varepsilon}(k)$ ,

where  $[\mathbf{x}_1(k), \mathbf{x}_2(k), \mathbf{x}_3(k)]$  represent machine tool, datum and fixture errors, respectively).

Aggregating error enables us to focus on the process with base errors only and thereby significantly reduces process and design variables in tolerance synthesis. The aggregated errors  $\mathbf{u}(k)$  and noise term  $\boldsymbol{\varepsilon}(k)$  are all assumed to follow multivariate normal distribution.

It should be noted that reducing model dimension can also be achieved by investigating the linear dependency among columns in the matrix  $\mathbf{\Gamma}_j$ , e.g., through diagnosability analysis (Zhou *et al.*, 2003). We adopt the error equivalence methodology because of two reasons. First of all, the machining process involves multiple types of errors as opposed to multiple error patterns from individual error sources (e.g., multiple fault patterns of the fixture error). Secondly, it is a more engineering driven approach, i.e., direct modeling the kinematic relationships among multiple error sources. The method assists more engineering insights, e.g., error cancellation effect discussed in Wang and

Huang, 2006. Using Eqn. (2.1), the variance-covariance matrix of the feature  $j$  can be derived as Eqn. (2.2). The  $\Sigma_{\mathbf{u}(k)}$  and  $\Sigma_{y_j}$  are variance-covariance matrix for process variables and deviation of feature  $j$ , respectively.

$$(\Sigma_{y_j}) = \Gamma_j (\Sigma_{\mathbf{u}(k)}) \Gamma_j^T + \sigma_\varepsilon^2 \mathbf{I}. \quad (2.2)$$

Since  $\text{diag}(\Sigma_{y_j})$  can be directly related with tolerance (e.g.,  $\pm 3\sigma$  as a measure of tolerance range), final tolerance stackup can be obtained by extracting the diagonal term  $\text{diag}(\Sigma_{y_j})$  from Eqn. (2.2).

With the tolerance stackup model, we can conduct equivalence error based simultaneous optimal tolerance allocation. The objective of optimal tolerance allocation is to allocate tolerances for process variables that can meet the design specification with minimum manufacturing cost. Denote process variables  $(\mathbf{u}(1)^T, \dots, \mathbf{u}(k)^T)^T$  as  $\Theta$  and their standard deviations as  $\sigma_\Theta = (\sigma_{\mathbf{u}(1)}, \dots, \sigma_{\mathbf{u}(k)})^T$ . The variances of product features are linear combinations of  $\sigma_\Theta^2$  from the result of  $\text{diag}(\Sigma_{y_j})$ , which can be denoted as  $\mathbf{C}^T \sigma_\Theta^2$ . The variance of dimensions, denoted as  $\mathbf{c}^T \sigma_\Theta^2$  can be derived from  $\mathbf{C}^T \sigma_\Theta^2$ . Since larger process tolerance for dimensions will reduce the manufacturing cost, we can maximize  $\mathbf{c}^T \sigma_\Theta^2$  given design specifications for the product tolerance and physical constraints:

$$\begin{aligned} & \text{Max } \mathbf{c}^T \sigma_\Theta^2, \text{ maximize the component tolerance;} \quad s.t. \\ & \mathbf{C}^T \sigma_\Theta^2 \leq \mathbf{b}_1, \text{ constrains from design specification} \quad (2.3) \\ & \mathbf{0} < \sigma_\Theta \leq \mathbf{b}_2, \text{ practical constraints of tooling} \\ & \mathbf{F}^c > 0, \text{ static equilibrium constraint} \end{aligned}$$

where  $\mathbf{F}^c$  is the reaction force between workpiece and locator and is determined by clamping forces. The static equilibrium constraint ensures the workpiece maintaining contact with all the locators (Cai, *et al.*, 1997). It should be noted that the tolerances are assigned to aggregated error sources. We could further distribute tolerances to individual error sources based on the error equivalence model given in Appendix A.

### 2.1.2 Error Equivalence Based Global Process Design Optimization

The tolerance stackup is determined not only by the magnitudes of error sources (measured by standard deviations of process variables in Section 2.1.1), but also by the process design, in particular, spatial layout of process variables. In a machining process, the layout of fixture locators has been shown to impact tolerance stackup with a 2-D example in Huang and Shi, 2003. But global optimization of process design was not studied therein. The main reason is that there is no unique solution for allocating tolerances to all process variables.

To overcome the challenge, we transform all error sources into equivalent amount of fixture locator errors. Then the process design variables are just positions of fixture locators (i.e.,  $\mathbf{f}_i$ 's). To explore the response surface of tolerance stackup under process design alternatives, we adopt the methodology of computer experiments design. The main reason is that the tolerance synthesis involves heavy symbolic computational load if we explore all possible fixture layouts. The lacking of random error in the deterministic computer tolerance simulation also leads to the consideration of computer experiments

against the other traditional regression analysis. And the computer experiments design will assist to establish a surrogate prediction model and to search the optimal process design.

We search the optimal tolerance allocation based on a Kriging model (Matheron, 1963; Journel and Huibregts, 1978; Cressie, 1993, and Sacks, *et al.*, 1989), which depicts the relationship between the input variables (e.g. fixture layout) and the tolerance stackup. Kriging model has advantage over other interpolation methods because it is more flexible and weights are not selected according to certain arbitrary rule (Li and Rizos, 2005). The Kriging model consists of a polynomial term  $\mathbf{f}^T(\mathbf{w})\boldsymbol{\beta}$  and a stochastic process  $Z(\mathbf{w})$  :

$$Y(\mathbf{w}) = \mathbf{f}^T(\mathbf{w})\boldsymbol{\beta} + Z(\mathbf{w}), \quad (2.4)$$

where  $Y(\mathbf{w})$  is the response (in our study, it represents tolerance assigned to the features) at the scaled input site  $\mathbf{w} = (w_1, \dots, w_d)$ , and  $d$  is the number of design variables. Note here we denote the untried site by  $\mathbf{w}$ , while the aforementioned  $\mathbf{s}_i$ 's are tried sites. The stochastic process  $Z(\cdot)$  is assumed to be Gaussian with zero-mean and a covariance between  $Z(\mathbf{w}_1)$  and  $Z(\mathbf{w}_2)$  at any two input sites  $\mathbf{w}_1$  and  $\mathbf{w}_2$ , i.e.,

$$\text{Cov}(\mathbf{w}_1, \mathbf{w}_2) = \sigma^2 R(\mathbf{w}_1, \mathbf{w}_2), \text{ where } R(\mathbf{w}_1, \mathbf{w}_2) \text{ is a correlation function of the responses.}$$

A review of prediction and estimation of Kriging model is given in Appendix B.

The structure of the polynomial term  $\mathbf{f}^T(\mathbf{w})\boldsymbol{\beta}$  and the correlation function in the stochastic process  $Z(\mathbf{w})$  should be determined first. According to Welch *et al.*, 1992, more elaborate polynomial terms offer little advantage in prediction. So we set a constant  $\beta$  for the polynomial term. For the structure of the correlation function, we choose power

exponential family correlation function that is the most popular in the computer experiments literature. It is given by the product of stationary one dimensional correlations as  $R(\mathbf{w}_1, \mathbf{w}_2) = \prod_{j=1}^d \exp(-\theta_j |w_{1j} - w_{2j}|^{p_j})$ , where  $0 \leq p_j \leq 2$ ,  $\theta_j \geq 0$ . We choose  $p_j=2$  because the correlation function with  $p_j=2$  produces smoother stochastic processes (Sacks, *et al.*, 1989). In a two-stage machining process, for instance, we have totally  $d=12$  design variables. Then the unknown parameters in Kriging model include constant term  $\beta$ , the variance  $\sigma^2$  of the stochastic process, and  $\boldsymbol{\theta} = (\theta_1, \dots, \theta_{12})$ .

To construct a precise Kriging model, a “good” experimental design should be able to provide an overview of the response across the whole design region as well as precise response at certain input sites in which we are interested (e.g., the input site or fixture layout that yield the optimal tolerance stackup).

Searching such an experimental design involves a sequential procedure (Bernardo, *et al.*, 1992; William, *et al.*, 2000; and Gupta *et al.*, 2006). The sequential procedure is consisting of initial design and design and model refinement.

To make the initial design spreading over the whole design region, we choose the latin hypercube sampling (LHS). It is one of the most frequently used space filling design and it was introduced by McKay *et al.*, 1979. For each component of input sites, i.e.,  $w_j$ , we can use a uniform distribution across each interval.

For high dimensional case, only some of the LHS designs are truly space filling (Santner, *et al.*, 2003). Therefore, the initial model may not well predict true tolerance

responses at uncertain sites and must be refined. We first calculate the root mean square error of the predictor RMSE ( $\hat{y}(\mathbf{w})$ ) at some tested sites, which is square root of Eqn. (B5). If the RMSE turns out to be too large, we should include these sites into the experimental design sites. The selection of untried sites can be determined by LHS design following maximin criteria. Maximin design guarantees that no two tested points are too close to each other, so that all the tested points are spread over the allowable design region. It should be noted that Gupta *et al.*, 2006, developed a zoom-in criteria to refine the Kriging model, whereby contour plot approach was used to show the mean square error (MSE) over the whole design region. The areas on the contour plot that have “too large” MSE will be zoomed in and added more design points. We choose to estimate the RMSE on a set of maximin-LHS design sites in each refinement iteration instead of contour plot for the reasons that firstly, the input sites may have higher dimension whereas contour plot is not efficient to explore the high dimensional design space; and secondly, maximin-LHS based test points selection can effectively search the tested points spreading over the whole design region. The iterative model refinement steps are stated as:

- *Kriging model fitting.* In the  $i$ th iteration, construct the Kriging model based on  $n_i$  available experimental design  $\mathbf{S} = \{\mathbf{s}_1, \dots, \mathbf{s}_{n_i}\}$  with response data  $\mathbf{y}_s = \{y_1, \dots, y_{n_i}\}$ , i.e.,  $\hat{y}(\mathbf{w}) = \hat{\boldsymbol{\beta}} + \mathbf{r}^T(\mathbf{w})_{n_i \times 1} \mathbf{R}_{n_i \times n_i}^{-1} (\mathbf{y}_s - \mathbf{e}_{n_i} \hat{\boldsymbol{\beta}})$ , where  $\mathbf{e}_{n_i}$  is the all-one vector of length  $n_i$ .  
 $i=0, 1, 2, \dots$

- *Model refinement.* Calculate RMSE at test points generated by maximin-LHS design and add the points that yield large RMSE to the experimental design. Let  $i \leftarrow i+1$  and repeat these procedures.

We can stop the model refinement when maximum response values do not vary significantly with iterations and the RMSE in the whole possible region is not too large (Gupta, *et al.*, 2006).

## 2.2 Case Study

In this Section, we will use a two-stage machining process as an example to illustrate error equivalence based tolerance synthesis and global process design optimization. Since a multistage process consists of operations with and without datum changes (the latter is simpler case), the two-stage example can be easily extended to a general case.

### 2.2.1 Illustrate the Approach Using a Multistage Machining Process

Figure 2.2 shows the part with features  $\mathbf{Y}_1 \sim \mathbf{Y}_7$ , where  $\mathbf{Y}_1$  and  $\mathbf{Y}_4$  are two planes, and  $\mathbf{Y}_2, \mathbf{Y}_3, \mathbf{Y}_5, \mathbf{Y}_6, \mathbf{Y}_7$  are cylindrical holes. The center of  $\mathbf{Y}_6$  is set to be the origin of global coordinate system (GCS). Part feature can be represented as, e.g.,  $\mathbf{Y}_1 = (0, 1, 0, 0, 131, 0)^T$ , where the first and last three numbers represent the orientation and position of  $\mathbf{Y}_1$ , respectively.

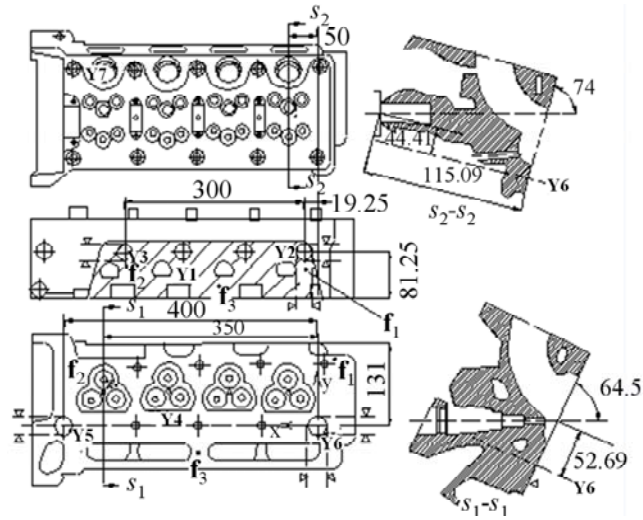


Figure 2.2 Workpiece and Locating Scheme (Wang, *et al.*, 2005)

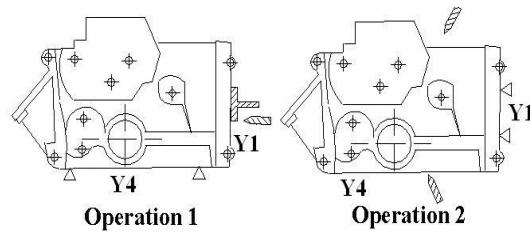


Figure 2.3 Operation Steps

The part goes through two operations, which are shown in Fig. 2.3. Firstly, use  $Y_4$ ,  $Y_5$ , and  $Y_6$  as datum surfaces to mill plane  $Y_1$  and drill two holes  $Y_2$  and  $Y_3$ . After that, the plane  $Y_1$  and two holes from operation one as datum surfaces to drill hole  $Y_7$ . In Fig. 1,  $f_1 \sim f_6$  show the locating positions on datum surfaces in each operation. The coordinates of fixture locators in operation one, e.g., is  $\mathbf{f}(1)_1 = (f(1)_{1x}, f(1)_{1y}, f(1)_{1z})^T = (-7, 109, 0)^T$ . Let  $\mathbf{x}_1(k)$ ,  $\mathbf{x}_2(k)$ ,  $\mathbf{x}_3(k)$  denote machine tool, datum and fixture errors respectively. The base error in this case study is fixture error, which can be represented as fixture locator

deviations, e.g.,  $(\Delta f(1)_{1z}, \Delta f(1)_{2z}, \Delta f(1)_{3z}, \Delta f(1)_{4y}, \Delta f(1)_{5y}, \Delta f(1)_{6x})^T$  in operation one. Next we will illustrate the whole procedure which contains two parts.

The first part is tolerance synthesis under specific fixture locating setting. For the tolerance stackup modeling, we only consider fixture and machine tool errors in operation one. However, the errors generated from this operation may cause datum error in operation two. Denote  $\mathbf{x}_1^*(k)$  and  $\mathbf{x}_2^*(k)$  as EFE due to machine tool and datum errors in operation  $k$ , respectively. Then  $\mathbf{u}(2) = \mathbf{x}_1^*(2) + \mathbf{x}_2^*(2) + \mathbf{x}_3(2)$ , where  $\mathbf{x}_2^*(2)$  is generated by  $\mathbf{u}(1)$ , as shown in Eqn. (A4). The final product feature deviation  $\mathbf{y}$  is

$$\mathbf{y} = \Gamma \begin{bmatrix} \mathbf{u}(1) \\ \mathbf{u}(2) \end{bmatrix} + \boldsymbol{\varepsilon} \quad , \quad (2.5)$$

where  $\Gamma = \begin{bmatrix} \Gamma_1 & \mathbf{0}_{6 \times 6} \\ \mathbf{0}_{6 \times 6} & \Gamma_7 \end{bmatrix}_{12 \times 12}$  and  $\mathbf{y} = [\mathbf{y}_1^T \ \mathbf{y}_7^T]^T$ . Matrices  $\Gamma_1$  and  $\Gamma_7$  are

$$\Gamma_1 = \begin{pmatrix} 0 & 0 & 0 & -0.0025 & 0.0025 & 0 \\ 0 & 0 & 0 & 0 & 0 & 0 \\ -0.00417 & -0.00417 & 0.00833 & 0 & 0 & 0 \\ 0 & 0 & 0 & -0.3275 & 0.3275 & -1 \\ 0 & 0 & 0 & -1 & 0 & 0 \\ -1.07476 & -0.10737 & 0.18333 & 0 & 0 & 0 \end{pmatrix}, \text{ and}$$

$$\Gamma_7 = \begin{pmatrix} -0.00143 & 0.00143 & 0 & -0.003 & 0.003 & 0 \\ -0.009 & -0.009 & 0.018 & 0 & 0 & 0 \\ 0.0043 & 0.0043 & -0.0086 & 0 & 0 & 0 \\ 0.26103 & -0.26103 & 0 & 0.27083 & -0.27083 & -1 \\ 0.715 & -0.49 & -1.225 & 0 & 0 & 0 \\ -0.7831 & -0.7831 & 1.5662 & 0.1025 & -1.1025 & 0 \end{pmatrix}.$$

By Eqn. (2.2), we obtain the final product features variance-covariance matrix  $\boldsymbol{\Sigma}_y$ . Denote the deviation of feature  $j$  by  $\mathbf{y}_j(k) = (\alpha_j, \beta_j, \gamma_j, x_j, y_j, z_j)^T$  (orientation deviation  $\alpha_j, \beta_j, \gamma_j$  and position deviation  $x_j, y_j, z_j$  in three directions). By extracting its diagonal term, we have the variances of features  $\mathbf{Y}_1$  and  $\mathbf{Y}_7$ , i.e.,

$$\sigma_{y_1}^2 = \left( \begin{array}{c} \frac{\sigma_{f(1)4y}^2}{160000} + \frac{\sigma_{f(1)5y}^2}{160000} + \sigma_\varepsilon^2 \\ \sigma_\varepsilon^2 \\ \frac{\sigma_{f(1)1z}^2}{57600} + \frac{\sigma_{f(1)2z}^2}{57600} + \frac{\sigma_{f(1)3z}^2}{14400} + \sigma_\varepsilon^2 \\ \sigma_{f(1)6x}^2 + \frac{17161\sigma_{f(1)4y}^2}{160000} + \frac{17161\sigma_{f(1)5y}^2}{160000} + \sigma_\varepsilon^2 \\ \sigma_{f(1)4y}^2 + \sigma_\varepsilon^2 \\ \frac{79192201\sigma_{f(1)1z}^2}{68558400} + \frac{808201\sigma_{f(1)2z}^2}{68558400} + \frac{121\sigma_{f(1)3z}^2}{3600} + \sigma_\varepsilon^2 \end{array} \right), \quad \text{and} \quad (2.6)$$

$$\sigma_{y_7}^2 = \left( \begin{array}{c} 1.15563 \times 10^{-6} \sigma_{f(1)4y}^2 + 1.15563 \times 10^{-6} \sigma_{f(1)5y}^2 + 2.05444 \times 10^{-6} \sigma_{f(2)1y}^2 + 2.05444 \times 10^{-6} \sigma_{f(2)2y}^2 \\ + 3.26928 \times 10^{-6} \sigma_{f(1)1z}^2 + 4.7259 \times 10^{-6} \sigma_{f(1)2z}^2 + 9 \times 10^{-6} \sigma_{f(2)4z}^2 + 9 \times 10^{-6} \sigma_{f(2)5z}^2 + \sigma_\varepsilon^2 \\ 8.1 \times 10^{-5} \sigma_{f(2)1y}^2 + 8.1 \times 10^{-5} \sigma_{f(2)2y}^2 + 3.24 \times 10^{-4} \sigma_{f(2)3y}^2 + 3.6565 \times 10^{-5} \sigma_{f(1)1z}^2 + 1.4063 \times 10^{-5} \sigma_{f(1)2z}^2 \\ + 5.625 \times 10^{-5} \sigma_{f(1)3z}^2 + \sigma_\varepsilon^2 \\ 1.849 \times 10^{-5} \sigma_{f(2)1y}^2 + 1.849 \times 10^{-5} \sigma_{f(2)2y}^2 + 7.396 \times 10^{-5} \sigma_{f(2)3y}^2 + 8.3467 \times 10^{-6} \sigma_{f(1)1z}^2 + 3.2101 \times 10^{-6} \sigma_{f(1)2z}^2 \\ + 1.284 \times 10^{-5} \sigma_{f(1)3z}^2 + \sigma_\varepsilon^2 \\ \sigma_{f(1)6x}^2 + \sigma_{f(2)6x}^2 + 0.01735 \sigma_{f(1)4y}^2 + 0.01735 \sigma_{f(1)5y}^2 + 0.06813 \sigma_{f(2)1y}^2 + 0.06813 \sigma_{f(2)2y}^2 + 0.00444 \sigma_{f(1)1z}^2 \\ + 0.07335 \sigma_{f(2)4z}^2 + 0.07335 \sigma_{f(2)5z}^2 + \sigma_\varepsilon^2 \\ 0.01563 \sigma_{f(1)4y}^2 + 0.76563 \sigma_{f(1)5y}^2 + 0.511225 \sigma_{f(2)1y}^2 + 0.2401 \sigma_{f(2)2y}^2 + 1.50063 \sigma_{f(2)3y}^2 + 0.0333 \sigma_{f(1)1z}^2 + \sigma_\varepsilon^2 \\ 0.61325 \sigma_{f(2)1y}^2 + 0.61325 \sigma_{f(2)2y}^2 + 2.45298 \sigma_{f(2)3y}^2 + 0.08809 \sigma_{f(1)1z}^2 + 0.394 \sigma_{f(1)2z}^2 + 0.2202 \sigma_{f(1)3z}^2 \\ + 0.01051 \sigma_{f(2)4z}^2 + 1.21551 \sigma_{f(2)5z}^2 + \sigma_\varepsilon^2 \end{array} \right).$$

The cylindrical hole  $\mathbf{Y}_7$  is critical for assembly in the subsequent operations. It is reasonable to set the tolerance for  $x$  and  $y$  positions of  $\mathbf{Y}_7$  as the final product tolerance, which correspond to the fourth and fifth components of  $\sigma_{y_7}^2$  in Eqn. (2.6), i.e.,  $\sigma_{x_7}^2$  and  $\sigma_{y_7}^2$ .

The objective is to maximize

$$0.5 \sigma_{x_7}^2 + 0.5 \sigma_{y_7}^2, \quad (2.7a)$$

where we assume equal importance of tolerances along two directions and therefore equal weights are assigned. Based on the vectorial dimension and tolerancing (VD&T) scheme

(Huang and Shi, 2003), the objective function (Eqn. (2.7a)) subjects to the constraints listed below:

$$\sigma_{\alpha_1}^2 \leq b_{\alpha_1}, \sigma_{\gamma_1}^2 \leq b_{\gamma_1}, \sigma_{y_1}^2 \leq b_{y_1} \text{ for } \mathbf{Y}_1, \quad (2.7b)$$

$$\text{and } \sigma_{\alpha_7}^2 \leq b_{\alpha_7}, \sigma_{\beta_7}^2 \leq b_{\beta_7}, \sigma_{\gamma_7}^2 \leq b_{\gamma_7}, \sigma_{x_7}^2 \leq b_{x_7}, \sigma_{y_7}^2 \leq b_{y_7}, \sigma_{z_7}^2 \leq b_{z_7} \text{ for } \mathbf{Y}_7.$$

Here  $b_{\beta_1}$ ,  $b_{x_1}$  and  $b_{z_1}$  need not to be considered because the orientation component of plane  $\mathbf{Y}_1$  is free in  $y$  direction, and the location component of the plane is free in  $x, z$  directions, respectively. As an example, we choose  $0.1 \text{radian}^2$  for  $b_{\alpha_1}$ ,  $b_{\gamma_1}$ ,  $b_{\alpha_7}$ ,  $b_{\beta_7}$ ,  $b_{\gamma_7}$ , and assign  $5 \text{mm}^2$  to  $b_{y_1}$ ,  $b_{x_7}$ ,  $b_{y_7}$ ,  $b_{z_7}$ , respectively. Set  $1.73 \text{mm}$  for all elements of  $\mathbf{b}_2$  in Eqn. (2.3). Then the tolerances or the maximum allowable standard deviations for the aggregated error sources are  $\sigma_{\Theta} = (0.01, 0.01, 0.01, 0.01, 1.415, 1.732, 1.732, 0.01, 1.135, 0.01, 0.01, 1.327)^T \text{mm}$ , and  $\mathbf{c}^T \sigma_{\Theta}^2 = 4.99 \text{mm}^2$ .

When more information is available at late stage of process design, e.g., the cost ratio between fixture and machine tool, we could further distribute the tolerances for aggregated error sources. For example, we could allocate 80% of tolerance band for aggregated EFE to machine tool error to reduce the cost of the major equipment. In operation one (no datum error occurs), we allocate 80% of  $\sigma_{\mathbf{u}(1)}$  to  $\sigma_{\mathbf{x}_1^*(1)}$ , i.e.,  $\sigma_{\mathbf{x}_1^*(1)} = 0.8 \sigma_{\mathbf{u}(1)}$ , where  $\sigma_{\mathbf{x}_3(1)}$  and  $\sigma_{\mathbf{x}_1^*(1)}$  denote the standard deviation of fixture error and EFE due to machine tool error in operation one, respectively. Variance-covariance matrix for machine tool error in the first stage will be

$$\Sigma_{\mathbf{x}_1(1)} = \mathbf{K}(1)_2^{-1} \Sigma_{\mathbf{x}_1^*(1)} (\mathbf{K}(1)_2^{-1})^T, \quad (2.8)$$

where  $\Sigma_{\mathbf{x}_1^*(1)} = \text{diag}(0.8^2 \sigma_{\mathbf{u}(1)}^2)$ . Appendix A gives the details of  $\mathbf{K}_1$  and  $\mathbf{K}_2$  matrices.

Solving Eqn. (2.8) and extracting  $\text{diag}(\boldsymbol{\Sigma}_{\mathbf{x}_1(1)})$ , we have  $\boldsymbol{\sigma}_{\mathbf{x}_1(1)} = (1.3856\text{mm}, 0.008\text{mm}, 0.0091\text{mm}, 2.7328 \times 10^{-5}\text{radian}, 8.1650 \times 10^{-5}\text{radian}, 0.0028\text{radian})$ , where the first three numbers represent the standard deviations of machine tool translational error, and the last three are corresponding to the standard deviations of the rotational error in three directions, respectively. Since the trajectory of machine tool head may vary significantly among different product features, we set the tightest tolerance for the machine tool error in all directions, i.e.,  $\boldsymbol{\sigma}_{\mathbf{x}_1(1)} = (8\mu\text{m}, 8\mu\text{m}, 8\mu\text{m}, 2.7328 \times 10^{-5}\text{radian}, 2.7328 \times 10^{-5}\text{radian}, 2.7328 \times 10^{-5}\text{radian})$ . For operation two, datum error is introduced from operation one. By Eqn. (A4), variance for EFE due to datum error is  $\text{diag}(\mathbf{K}\boldsymbol{\Sigma}_{\mathbf{u}(1)}\mathbf{K}^T) = \text{diag}(\boldsymbol{\Sigma}_{\mathbf{x}_2^*(2)}) = \boldsymbol{\sigma}_{\mathbf{x}_2^*(2)}^2 = (0.069\text{mm}^2, 1.1294\text{mm}^2, 0.5988\text{mm}^2, 0.00264\text{mm}^2, 0.0095\text{mm}^2, 1.7929\text{mm}^2)$ .

Further allocation of tolerance for datum error can be found by

$$\text{diag}(\mathbf{K}(2)_1 \boldsymbol{\Sigma}_{\mathbf{x}_2(2)} (\mathbf{K}(2)_1)^T) = \text{diag}(\boldsymbol{\Sigma}_{\mathbf{x}_2^*(2)}). \quad (2.9)$$

However, the solution for datum tolerances is not unique since  $\mathbf{K}_1$  is a  $6 \times 18$  matrix (Eqn. (A3)). Therefore, we can not simply obtain  $\text{diag}(\boldsymbol{\Sigma}_{\mathbf{x}_2(2)})$  by  $\text{diag}(\mathbf{K}(2)_1^{-1} \boldsymbol{\Sigma}_{\mathbf{x}_2^*(2)} (\mathbf{K}(2)_1^{-1})^T)$ .

Due to the characteristics of  $\mathbf{K}_1$ , it is necessary to first specify tolerance for one element of secondary datum surface and two elements of tertiary datum surface. Denote  $\mathbf{x}_2 = (\mathbf{v}_I, \mathbf{p}_I, \mathbf{v}_{II}, \mathbf{p}_{II}, \mathbf{v}_{III}, \mathbf{p}_{III})$ , where I, II, III represent primary, secondary and tertiary datum surfaces, respectively. The  $\mathbf{v}$  and  $\mathbf{p}$  represent rotational and translational error of the datum surfaces in three directions. (e.g.,  $v(2)_{Ix}$  represents the rotational error of primary datum surface in  $x$  direction in operation 2). Assign  $1 \times 10^{-9} \text{radian}^2$  to  $\sigma_{v(2)_{Iy}}^2$ ,  $1 \times 10^{-7} \text{radian}^2$  to  $\sigma_{v(2)_{Iy}}^2$ , and  $1 \times 10^{-6} \text{mm}^2$  to  $\sigma_{p(2)_{IIIx}}^2$ . Solving Eqn. (9) leads to  $\boldsymbol{\sigma}_{\mathbf{x}_2(2)} = (\sigma_{v(2)_{Ix}}, \sigma_{v(2)_{Iz}},$

$(\sigma_{p(2)_y}, \sigma_{v(2)_{lx}}, \sigma_{v(2)_{ly}}, \sigma_{p(2)_{lz}}, \sigma_{v(2)_{ly}}, \sigma_{v(2)_{lz}}, \sigma_{p(2)_{lx}}) = (0.0035\text{radian},$   
 $1.3995 \times 10^{-4}\text{radian}, 7.5\mu\text{m}, 2.473 \times 10^{-5}\text{radian}, 3.1623 \times 10^{-5}\text{radian}, 3.2\mu\text{m},$   
 $3.1623 \times 10^{-4}\text{radian}, 0.0221\text{radian}, 1\mu\text{m}).$

To distribute tolerances to fixture and machine tool errors in operation two, we have  $\sigma_{x_1^*(2)} = 0.8(\sigma_{u(2)} - \sigma_{x_2^*(2)}) = (1.1914\text{mm}, 0.00024\text{mm}, 0.4802\text{mm}, 0.0413\text{mm}, 0.0004\text{mm}, 0.4368\text{mm})$ . To calculate tolerance for machine tool error in operation 2, we have

$$\Sigma_{x_1(2)} = \mathbf{K}(2)_2^{-1} \Sigma_{x_1^*(2)} (\mathbf{K}(2)_2^{-1})^T. \quad (2.10)$$

Thus,  $\sigma_{x_1(2)}^2 = (0.4616\text{mm}^2, 0.6356\text{mm}^2, 4.0206\text{mm}^2, 0.00023\text{radian}^2, 1.8936 \times 10^{-8}\text{radian}^2, 0.0000158\text{radian}^2)$ . By setting equal tolerances for translational and rotational deviations in three directions, we obtain  $\sigma_{x_1(2)} = (0.6794\text{mm}, 0.6794\text{mm}, 0.6794\text{mm}, 0.000137\text{radian}, 0.000137\text{radian}, 0.000137\text{radian})$ .

Based on the work of first part, we can conduct global process design optimization within allowable fixture locating setting range. Recall that all the error sources have been transformed into EFE. Hence the input site  $\mathbf{w}$  is related to the fixture layout and can be obtained as follows. Under 3-2-1 locating scheme, only locators 1, 2, 3 in the example can be movable over the allowable design region since the positions of locators 4, 5, and 6 are fixed with locating holes. Each of locators 1, 2, and 3 can move on the primary datum plane in two directions. Therefore, there are twelve design variables involved in total for two machining processes, i.e.,  $\mathbf{\Omega} = (f(1)_{1x}, f(1)_{1y}, f(1)_{2x}, f(1)_{2y}, f(1)_{3x}, f(1)_{3y}, f(2)_{1x}, f(2)_{1z}, f(2)_{2x}, f(2)_{2z}, f(2)_{3x}, f(2)_{3z})$ . The allowable design region

for each design variables is summarized in Table 2.1. The input variables for  $\Omega$  are usually coded into  $[0, 1]^d$ . i.e.,  $\mathbf{w}$ , where,  $d=12$ ,  $0 \leq w_i \leq 1$ ,  $i = 1, 2, \dots, 12$ . Here we can choose uniform distribution within the  $[0, 1]^d$  interval.

Table 2.1 Design Variables Range under GCS (unit: mm)

Operation 1	$f(1)_{1x}$	$f(1)_{1y}$	$f(1)_{2x}$	$f(1)_{2y}$	$f(1)_{3x}$	$f(1)_{3y}$
Range	0~400	-10~130	0~400	-10~130	0~400	-10~130
Operation 2	$f(2)_{1x}$	$f(2)_{1z}$	$f(2)_{2x}$	$f(2)_{2z}$	$f(2)_{3x}$	$f(2)_{3z}$
Range	0~360	0~80	0~360	0~80	0~360	0~80

Since three locators have same allowable ranges, they may overlap each other when we generate design sites, this can be prevented by checking deterministic locating condition, i.e., the Jacobian matrix of the fixture layout should be of full rank (Cai, *et al.*, 1997). As mentioned in Section 2, the reaction force should be non-negative (we choose  $>0.5\text{kN}$  here) at the locating points so that the locators contact the workpiece.

Considering the feature dimensions of the workpiece and clamping limitations, we determine the resultant clamping force and torque at the origin as follow: for operation one,  $\mathbf{F}^A = (-52\text{kN}, -28\text{kN}, -25\text{kN})$ ,  $\mathbf{T}^A = (-10136\text{Nm}, 18300\text{Nm}, -4489\text{Nm})$ ; for operation two,  $\mathbf{F}^A = (-45\text{kN}, 294\text{kN}, 158\text{kN})$ ,  $\mathbf{T}^A = (-149\text{Nm}, 302\text{Nm}, -51\text{Nm})$ . In addition, the static constraint can help to reduce the number of optimal fixture layouts that correspond to the maximum value of  $\hat{y}$ .

Before selecting the initial design sites, we should determine the number of design sites. Number of points  $n_0$  for initial experimental design should be chosen to balance the experiment running time and fidelity of Kriging model. It was suggested (Bernardo *et al.*, 1992) that  $n_0$  should be chosen at most three times the number of unknown parameters in the Kriging model. For our EFE based tolerance study, we have totally 14 unknown parameters (12  $\theta_j$ 's, 1 constant  $\beta$ , and 1 process variance  $\sigma^2$ ). Thus, we should let  $n_0$  be at least 14 and no more than 42.

Here, we choose 16 points, which give rise to a  $16 \times 12$  maximin-LHS design. Unknown parameters in Kriging model can be estimated by maximum likelihood estimation (MLE) criterion, i.e., optimizing the objective function Eqn. (B1) in Appendix B. There are many searching algorithms available such as simplex search, pattern search methods, and Powell's conjugate direction search method. In our study, we choose Torczon pattern search method, because Torczon, 1997, proved that pattern search methods can converge to stationary points. Furthermore, pattern search method can easily be extended for constrained optimization. After the initial design, we choose 52 maximin-LHS design sites for model refinement iteration (at least three times number of unknown parameters in the Kriging model). We choose the extra design sites whose RMSE's are larger than 85% of the largest RMSE of the total tested sites. In our experiment, the largest RMSE of tested sites is around 0.224, the RMSE test gives rise to another 7 points (where  $RMSE > 0.224 * 0.85 = 0.19$ ) to be added to the design.

When maximum response values do not vary significantly with iterations (Gupta, *et al.*, 2006) and the RMSE in the whole possible region is not too large, we can stop the refinement steps, and obtain a model with  $\hat{\beta} = 4.6957$ ,  $\hat{\theta} = (0.1, 0.85, 0.1, 0.1, 0.725, 0.1, 1.6, 0.6, 0.1, 0.1, 0.6, 0.6)$ . The optimal solution  $\mathbf{w}^*$  that yields maximum tolerance  $\hat{y}$  in the Kriging model can be obtained by simplex search, i.e.,  $\mathbf{w}^* = (0.4375, 0.4688, 0.1875, 0.1016, 0.7344, 0.3438, 0, 0.4219, 0.7813, 0.7344, 0.4531, 0.5469)^T$ . The corresponding fixture layout is  $\mathbf{\Omega}^* = (175, 55.625, 75, 4.2188, 293.75, 38.125, 0, 33.75, 281.25, 58.75, 163.125, 43.75)^T$  mm, with  $\hat{y}(\mathbf{w}^*) = 5.029\text{mm}^2$ , and  $\text{RMSE}(\hat{y}(\mathbf{w}^*)) = 0.0872\text{mm}^2$ . The yielded reaction forces from six locators are  $\mathbf{F}^c = (18.2633\text{kN}, 21.3421\text{kN}, 12.7536\text{kN}, 22.0025\text{ kN}, 5.6110\text{ kN}, 25.3354\text{ kN})$  for operation one, and  $\mathbf{F}^c = (0.5672\text{ kN}, 0.6833\text{ kN}, 0.8252\text{kN}, 0.6773\text{kN}, 0.7525\text{kN}, 0.6631\text{kN})$  for operation two. Based on these optimal design variables, we can implement the tolerance synthesis by the similar approach presented in Section 2.1.

### 2.2.2 Remark on Sensitivity Analysis of the Optimal Process Design

The sensitivity analysis is to study the robustness of the optimal fixture layout obtained. The idea of the sensitivity analysis is to study impact of subtle perturbation at the optimal design point on the response, i.e., to evaluate sensitivity

coefficients  $\left. \frac{\partial \hat{y}(\mathbf{w})}{\partial w_i} \right|_{\mathbf{w}=\text{Optimal desin variable}}$ ,  $i = 1, \dots, 12$ . Through analysis of these values, we can

find out the sensitive direction along which small movement of locators has significant

impact on the tolerance stackup. Sensitivity directions could provide guidelines for fixture design, e.g., we should set tight tolerance for fixture locator assembly along these directions. After computation, at the optimal design point, the sensitivity coefficients are (0.005, 0.0164, 0.0119, 0.0056, -0.0272, 0.0030, 0.3202, -0.0119, -0.0043, -0.0216, 0.0081, 0.0184). We can see that locator 1 in operation 2 has a relatively large sensitivity coefficient in  $x$  direction, and sensitivity coefficient is relatively large at locator 3 in  $x$  direction in operation 2. The assembly tolerance for these directions should be stricter than other directions.

### 2.3 Chapter Summary

This Chapter develops a new process design and optimization method to seek an efficient and optimal process tolerance design for multistage machining processes. The idea is to reduce the design space in optimization problem by developing a tolerance stackup model in which multiple error sources are aggregated into one base error through error equivalence transformation. The model based process tolerance design and optimization has a hierarchical structure, i.e., assign the tolerances to the aggregated/bundled error sources first and then distribute them to individual error sources at each stage through cost analysis. Compared with a flat structure by which tolerances are directly assigned to individual error sources, the hierarchical structure can avoid dramatic, complete change of tolerance allocation and process design due to subtle change of cost functions.

In the mean time, the proposed method also searches optimal tolerance stackup as well as process design by exploring all possible combinations of process design variables. Computer experiments method is employed to establish the surrogate model for tolerance stackup prediction and optimal process design. Space filling method (LHS along with maximin criterion) will first generate random design points and we obtain optimal tolerance stackup at each design point. A Kriging model is then derived and refined by sequentially adding more design points into the regions with high uncertainty. One can further distribute the assigned tolerance for base errors among individual error sources when more process information is available. We illustrate the approach through a two-stage machining process where all errors were transformed to equivalent fixture errors. It has been demonstrated that consideration of error equivalence mechanism could significantly relieve the computation load of tolerance optimization problem and Kriging model fitting. The robustness of optimal tolerance to process variation is evaluated by a sensitivity analysis. In the two-stage machining process, we analyze the sensitivity of tolerance stackup to the optimal layout of fixture locators. The sensitivity analysis shows that the optimal design is more sensitive along some direction. The results provide a guideline to design the manufacturing process.

## Chapter 3

### Diagnose Multiple Variation Sources under Variation Equivalence

This Chapter aims to improve the root cause diagnosis by utilizing the variation equivalence phenomenon. There are deviational error equivalences among different individual error sources, i.e., the fixture error, machine tool error and datum error can generate the same deviation pattern on product feature. In the variation point of view, the equivalent phenomena also happen among the variations of different error sources under certain conditions. This makes the process diagnosis and root cause identification of multiple variation sources more challenging. Meanwhile, based on error equivalence, we can study the equivalent properties among different variation sources by connecting the physical equivalence phenomena to mathematical formulation. Moreover, through exploring possible equivalent variations cases, we can construct an equivalent variation patterns library, which are useful for variation patterns mapping in process fault diagnosis. All of these will help to improve root cause identification of process fault among multiple variation sources.

This Chapter is organized as follows. Section 3.1 introduces the concept of variation equivalence and constructs the equivalent variation patterns library. The diagnosis and root cause identification under variation equivalence is presented in

Section 3.2. The Section 3.3 verifies the approach by illustrating a case study. Conclusion is given in Section 3.4.

### 3.1 Concept of Variation Equivalence and Equivalent Variation Patterns Library

Previous application of error equivalence methodology on process diagnosis and root cause identification has focused on diagnosing and distinguishing process deviation (mean shift). For instance, Wang *et al.*, 2006 utilized the EFE concept and the error compensating error strategy to improve the process diagnosis and root cause identification. However, besides deviation, process faults also manifest themselves as variation increases. Thus, it is also possible that equivalence occur in terms of variation. We can call this phenomenon as variation equivalence, which concerns that different error sources may result in identical product feature variation pattern. This Section will give the definition of variation equivalence and explore the possible variation equivalence cases in machining process, which are used to construct the equivalent variation patterns library.

#### 3.1.1 Definition of Variation Equivalence

The definition of variation equivalence is that an identical part feature variation pattern can be generated by different process variation sources.

To understand the definition, we can use a simple machining process to explain. The operation is to mill the top surface of the block part, which is shown in Fig. 3.1. If

machine tool translational error in y direction has large variation, it will cause large variation of the part top surface position. The large variation of the top surface position can also be caused by large variation of the primary datum surface (the bottom surface) position. Similarly, if the two locators that are in touch with the primary datum surface are loose and have positive correlation, the part top surface would have the same variation pattern too. Denote the part feature as  $\mathbf{y}$  (in this case it is the top surface position). And denote the part feature variation caused by variation source  $s$  as  $\text{Var}(\mathbf{y}_s)$ , where  $s = \mathbf{f}, \mathbf{m},$  and  $\mathbf{d}$ , corresponding to fixture error, machine tool error and datum error, respectively. We will have  $\text{Var}(\mathbf{y}) = \text{Var}(\mathbf{y}_f) = \text{Var}(\mathbf{y}_d) = \text{Var}(\mathbf{y}_m)$ .

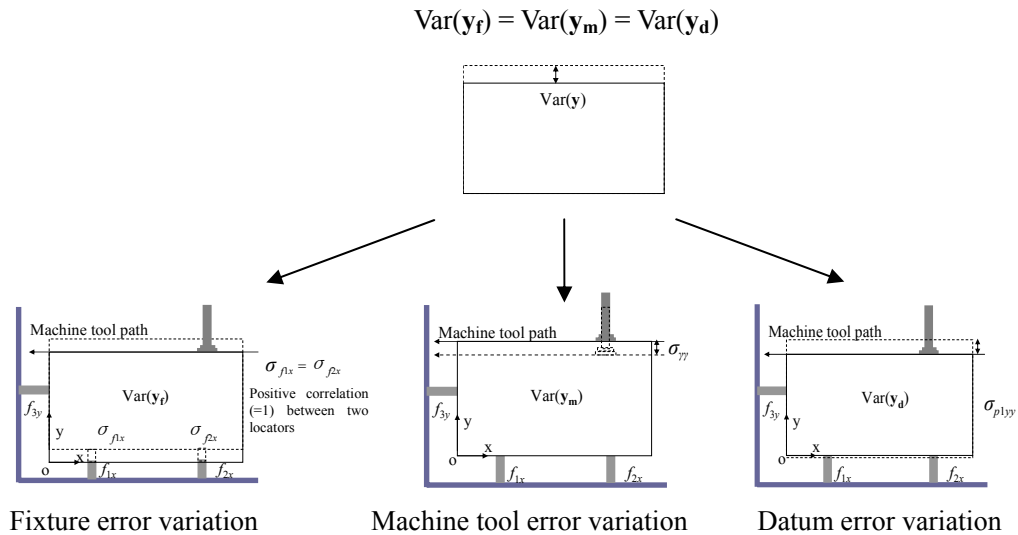


Figure 3.1 A 2-D Machining Process Example of Variation Equivalence

### 3.1.2 Equivalent Covariance Structure Analysis and Library

Based on the variation equivalence concept, we can explore possible equivalent product feature variation patterns and link physical explanations of variation equivalence

to mathematical formulation and analysis. Recall that the error equivalence based causality process model  $\mathbf{y}_j(k) = \mathbf{\Gamma}_j \mathbf{u}(k) + \boldsymbol{\varepsilon}(k)$  (Wang, Huang, and Katz, 2005) presents the relationship between product feature deviation  $\mathbf{y}_j(k)$  and integrated process equivalent fixture errors (EFE)  $\mathbf{u}(k)$  in  $k$ th stage. And  $\mathbf{u}(k) = \sum_i \mathbf{x}_i^*(k)$ . The  $\mathbf{x}_i^*(k)$ 's are the equivalent fixture error transformed from different individual error sources, e.g., from datum error and machine tool error  $\mathbf{x}_1^* = \mathbf{K}_2 \mathbf{x}_1$  and  $\mathbf{x}_2^* = \mathbf{K}_1 \mathbf{x}_2$ , (Wang, *et al.*, 2005), where the  $\mathbf{K}_1$  and  $\mathbf{K}_2$  matrices are error equivalence modeling transformation matrices in Appendix A. Taking the covariance of this model, we can obtain the covariance structures of part feature and those of integrated process equivalent fixture error

$$(\boldsymbol{\Sigma}_{\mathbf{y}_j}) = \mathbf{\Gamma}_j (\boldsymbol{\Sigma}_{\mathbf{u}(k)}) \mathbf{\Gamma}_j^T + \sigma_\varepsilon^2 \mathbf{I}. \quad (3.1)$$

The Eqn. (3.1) denotes the relationship between the covariance structure of process EFE and that of part feature. Thus we can connect the part feature variation patterns to the variation patterns of EFE. Since our task is to develop an efficient approach for root cause identification among multiple variation sources under variation equivalence, studying  $\boldsymbol{\Sigma}_{\mathbf{u}(k)}$  instead of  $\boldsymbol{\Sigma}_{\mathbf{y}_j}$  will more helpful to our research. Thus we will explore possible equivalent product feature variation patterns that are connected to  $\boldsymbol{\Sigma}_{\mathbf{u}(k)}$ . Taking the covariance for both sides of the error equivalence transformation model (Eqns. (A1)~(A3)), we can obtain the covariance structures of EFE due to machine tool error and datum error as  $\mathbf{K}_2 \boldsymbol{\Sigma}_{\mathbf{x}_1} \mathbf{K}_2^T$  and  $\mathbf{K}_1 \boldsymbol{\Sigma}_{\mathbf{x}_2} \mathbf{K}_1^T$ . Specifically, the general covariance structures for 2-D case are:

$$\mathbf{\Sigma}_M = \begin{pmatrix} \sigma_{yy} + f_{1x}^2 \sigma_{\gamma\gamma} & \sigma_{yy} + f_{1x} f_{2x} \sigma_{\gamma\gamma} & \sigma_{xy} - f_{1x} f_{3y} \sigma_{\gamma\gamma} \\ \sigma_{yy} + f_{1x} f_{2x} \sigma_{\gamma\gamma} & \sigma_{yy} + f_{2x}^2 \sigma_{\gamma\gamma} & \sigma_{xy} - f_{2x} f_{3y} \sigma_{\gamma\gamma} \\ \sigma_{xy} - f_{1x} f_{3y} \sigma_{\gamma\gamma} & \sigma_{xy} - f_{2x} f_{3y} \sigma_{\gamma\gamma} & \sigma_{xx} + f_{3y}^2 \sigma_{\gamma\gamma} \end{pmatrix}, \quad (3.2a)$$

and

$$\mathbf{\Sigma}_D = \begin{pmatrix} \sigma_{p1yy} + f_{1x}^2 \sigma_{v1xx} & \sigma_{p1yy} + f_{1x} f_{2x} \sigma_{v1xx} & \sigma_{\varepsilon\varepsilon} \\ \sigma_{p1yy} + f_{1x} f_{2x} \sigma_{v1xx} & \sigma_{p1yy} + f_{2x}^2 \sigma_{v1xx} & \sigma_{\varepsilon\varepsilon} \\ \sigma_{\varepsilon\varepsilon} & \sigma_{\varepsilon\varepsilon} & \sigma_{p2xx} + f_{3y}^2 \sigma_{v2yy} \end{pmatrix}, \quad (3.2b)$$

where  $f_{1x}$ ,  $f_{2x}$  and  $f_{3y}$  denote the three locators coordinate under part coordinate system (PCS), with indices 1, 2 representing the two in touch with primary datum surface, and 3 for the one on secondary datum surface. The  $\sigma_{\gamma\gamma}$  is the variance of machine tool rotational error,  $\sigma_{xx}$  is the variance of machine tool translational error in x direction, and  $\sigma_{yy}$  is the variance of machine tool translational error in y direction. And  $\sigma_{v1xx}$  is the variance of primary datum normal vector error in x direction;  $\sigma_{p1yy}$  is the variance of primary datum surface position in y direction,  $\sigma_{v2yy}$  is the variance of secondary datum normal vector error in y direction,  $\sigma_{p2xx}$  is the variance of secondary datum surface position in y direction. The details with regarding to the derivation of Eqns. (3.2a) and (3.2b) are illustrated in the Appendix C.

These two equations connect the physical meaning of variation patterns in machining processes to the mathematical explanations. By analyzing  $\mathbf{\Sigma}_M$  and  $\mathbf{\Sigma}_D$  under possible faulty/malfunction conditions, we may construct the equivalent covariance patterns library and obtain some information of how the covariance patterns change under different variation sources settings. For simplicity, we use a block part to explore all the possible variation equivalence cases between machine tool error and datum error. The

product feature here is the top surface of the block part, with the process of milling the top surface. The library patterns are listed as follows:

- *Faulty condition 1: product feature (top surface) has large normal vector variation.*

In this case, we can see from Fig. 3.2 that the block part top surface normal vector will have large variation. This product feature variation pattern can be generated from large variation of machine tool angle error as well as from large variation of primary datum surface normal vector error. The covariance matrices of EFE due to machine tool error and due to datum error are given by Eqn. (3.3a) and (3.3b). Those subscripts with letter “N” denote the normal condition values.

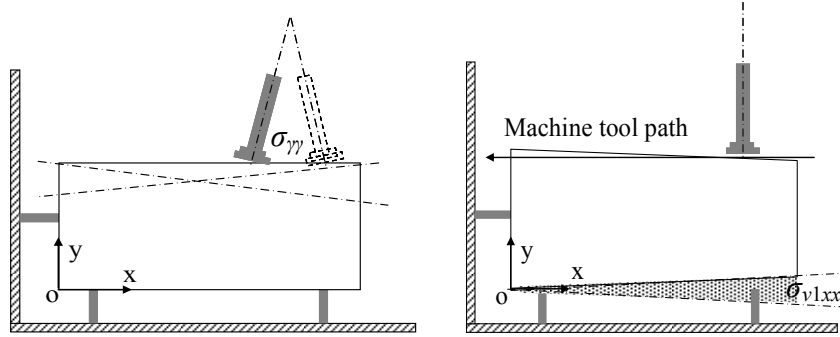


Figure 3.2 Variation Equivalence of Faulty Condition 1

$$\Sigma_{\mathbf{M}} = \begin{pmatrix} \sigma_{yyN} + f_{1x}^2 \sigma_{\gamma\gamma} & \sigma_{yyN} + f_{1x} f_{2x} \sigma_{\gamma\gamma} & \sigma_{xy} - f_{1x} f_{3y} \sigma_{\gamma\gamma} \\ \sigma_{yyN} + f_{1x} f_{2x} \sigma_{\gamma\gamma} & \sigma_{yyN} + f_{2x}^2 \sigma_{\gamma\gamma} & \sigma_{xy} - f_{2x} f_{3y} \sigma_{\gamma\gamma} \\ \sigma_{xy} - f_{1x} f_{3y} \sigma_{\gamma\gamma} & \sigma_{xy} - f_{2x} f_{3y} \sigma_{\gamma\gamma} & \sigma_{xxN} + f_{3y}^2 \sigma_{\gamma\gamma} \end{pmatrix}, \quad (3.3a)$$

$$\Sigma_{\mathbf{D}} = \begin{pmatrix} \sigma_{p1yyN} + f_{1x}^2 \sigma_{v1xx} & \sigma_{p1yyN} + f_{1x} f_{2x} \sigma_{v1xx} & \sigma_{\varepsilon\varepsilon} \\ \sigma_{p1yyN} + f_{1x} f_{2x} \sigma_{v1xx} & \sigma_{p1yyN} + f_{2x}^2 \sigma_{v1xx} & \sigma_{\varepsilon\varepsilon} \\ \sigma_{\varepsilon\varepsilon} & \sigma_{\varepsilon\varepsilon} & \sigma_{p2xxN} + f_{3y}^2 \sigma_{v2yy} \end{pmatrix}. \quad (3.3b)$$

- *Faulty condition 2: there is large positional variation in x direction.* The Fig 3.3 illustrates this case. There will be no negative impact on milling the top surface in this case. However, if the operation is to drill a hole in the top surface, the impact will be significant. The covariance matrices of EFE due to machine tool error and due to datum error are given by Eqn. (3.4a) and Eqn. (3.4b).

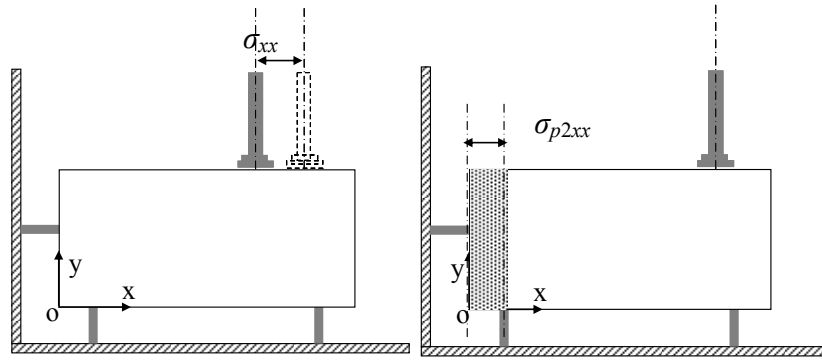


Figure 3.3 Variation Equivalence of Faulty Condition 2

$$\Sigma_{\mathbf{M}} = \begin{pmatrix} \sigma_{yyN} + f_{1x}^2 \sigma_{\gamma\gamma N} & \sigma_{yyN} + f_{1x} f_{2x} \sigma_{\gamma\gamma N} & \sigma_{xyN} - f_{1x} f_{3y} \sigma_{\gamma\gamma N} \\ \sigma_{yyN} + f_{1x} f_{2x} \sigma_{\gamma\gamma N} & \sigma_{yyN} + f_{2x}^2 \sigma_{\gamma\gamma N} & \sigma_{xyN} - f_{2x} f_{3y} \sigma_{\gamma\gamma N} \\ \sigma_{xyN} - f_{1x} f_{3y} \sigma_{\gamma\gamma N} & \sigma_{xyN} - f_{2x} f_{3y} \sigma_{\gamma\gamma N} & \sigma_{xx} + f_{3y}^2 \sigma_{\gamma\gamma N} \end{pmatrix}, \quad (3.4a)$$

$$\Sigma_{\mathbf{D}} = \begin{pmatrix} \sigma_{p1yyN} + f_{1x}^2 \sigma_{v1xxN} & \sigma_{p1yyN} + f_{1x} f_{2x} \sigma_{v1xxN} & \sigma_{\varepsilon\varepsilon} \\ \sigma_{p1yyN} + f_{1x} f_{2x} \sigma_{v1xxN} & \sigma_{p1yyN} + f_{2x}^2 \sigma_{v1xxN} & \sigma_{\varepsilon\varepsilon} \\ \sigma_{\varepsilon\varepsilon} & \sigma_{\varepsilon\varepsilon} & \sigma_{p2xx} + f_{3y}^2 \sigma_{v2yyN} \end{pmatrix}. \quad (3.4b)$$

- *Faulty condition 3: there is large positional variation in y direction.* This faulty condition will significantly affect the product feature's displacement, which is explained by Fig. 3.4. The covariance matrices of EFE due to machine tool error and due to datum error are given by Eqn. (3.5a) and (3.5b).

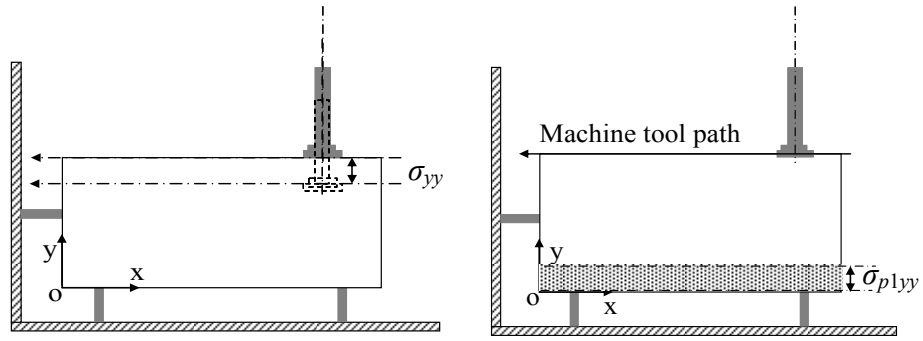


Figure 3.4 Variation Equivalence of Faulty Condition 3

$$\Sigma_{\mathbf{M}} = \begin{pmatrix} \sigma_{yy} + f_{1x}^2 \sigma_{\gamma\gamma N} & \sigma_{yy} + f_{1x} f_{2x} \sigma_{\gamma\gamma N} & \sigma_{xyN} - f_{1x} f_{3y} \sigma_{\gamma\gamma N} \\ \sigma_{yy} + f_{1x} f_{2x} \sigma_{\gamma\gamma N} & \sigma_{yy} + f_{2x}^2 \sigma_{\gamma\gamma N} & \sigma_{xyN} - f_{2x} f_{3y} \sigma_{\gamma\gamma N} \\ \sigma_{xyN} - f_{1x} f_{3y} \sigma_{\gamma\gamma N} & \sigma_{xyN} - f_{2x} f_{3y} \sigma_{\gamma\gamma N} & \sigma_{xxN} + f_{3y}^2 \sigma_{\gamma\gamma N} \end{pmatrix}, \quad (3.5a)$$

$$\Sigma_{\mathbf{D}} = \begin{pmatrix} \sigma_{p1yy} + f_{1x}^2 \sigma_{v1xxN} & \sigma_{p1yy} + f_{1x} f_{2x} \sigma_{v1xxN} & \sigma_{\varepsilon\varepsilon} \\ \sigma_{p1yy} + f_{1x} f_{2x} \sigma_{v1xxN} & \sigma_{p1yy} + f_{2x}^2 \sigma_{v1xxN} & \sigma_{\varepsilon\varepsilon} \\ \sigma_{\varepsilon\varepsilon} & \sigma_{\varepsilon\varepsilon} & \sigma_{p2xxN} + f_{3y}^2 \sigma_{v2yyN} \end{pmatrix}. \quad (3.5b)$$

- *Faulty condition 4: part feature has large variations of both normal vector and position in y direction.* The Fig. 3.5, Eqn. (3.6a) and (3.6b) explain this case physically and mathematically.

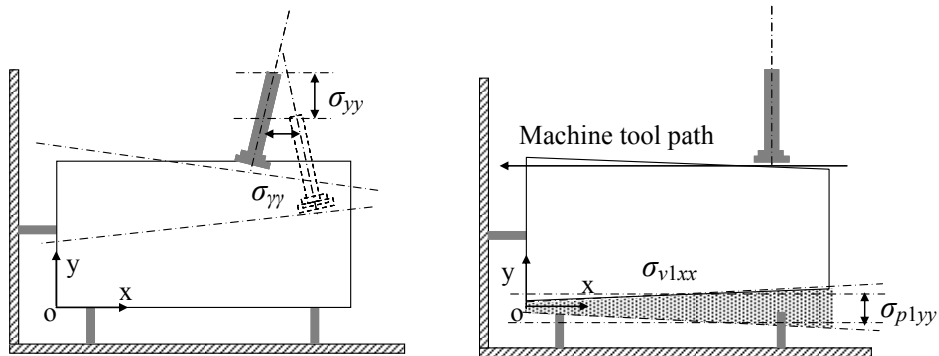


Figure 3.5 Variation Equivalence of Faulty Condition 4

$$\Sigma_{\mathbf{M}} = \begin{pmatrix} \sigma_{yy} + f_{1x}^2 \sigma_{\gamma\gamma} & \sigma_{yy} + f_{1x} f_{2x} \sigma_{\gamma\gamma} & \sigma_{xy} - f_{1x} f_{3y} \sigma_{\gamma\gamma} \\ \sigma_{yy} + f_{1x} f_{2x} \sigma_{\gamma\gamma} & \sigma_{yy} + f_{2x}^2 \sigma_{\gamma\gamma} & \sigma_{xy} - f_{2x} f_{3y} \sigma_{\gamma\gamma} \\ \sigma_{xy} - f_{1x} f_{3y} \sigma_{\gamma\gamma} & \sigma_{xy} - f_{2x} f_{3y} \sigma_{\gamma\gamma} & \sigma_{xxN} + f_{3y}^2 \sigma_{\gamma\gamma} \end{pmatrix}, \quad (3.6a)$$

$$\Sigma_{\mathbf{D}} = \begin{pmatrix} \sigma_{p1yy} + f_{1x}^2 \sigma_{v1xx} & \sigma_{p1yy} + f_{1x} f_{2x} \sigma_{v1xx} & \sigma_{\varepsilon\varepsilon} \\ \sigma_{p1yy} + f_{1x} f_{2x} \sigma_{v1xx} & \sigma_{p1yy} + f_{2x}^2 \sigma_{v1xx} & \sigma_{\varepsilon\varepsilon} \\ \sigma_{\varepsilon\varepsilon} & \sigma_{\varepsilon\varepsilon} & \sigma_{p2xxN} + f_{3y}^2 \sigma_{v2yy} \end{pmatrix}. \quad (3.6b)$$

- *Faulty condition 5: part feature has large variations of both normal vector and position in x direction.* The Fig. 3.6 illustrates this case. We can see that this case is similar to Faulty condition 1. The covariance matrices of EFE due to machine tool error and due to datum error are given by Eqn. (3.7a) and (3.7b).

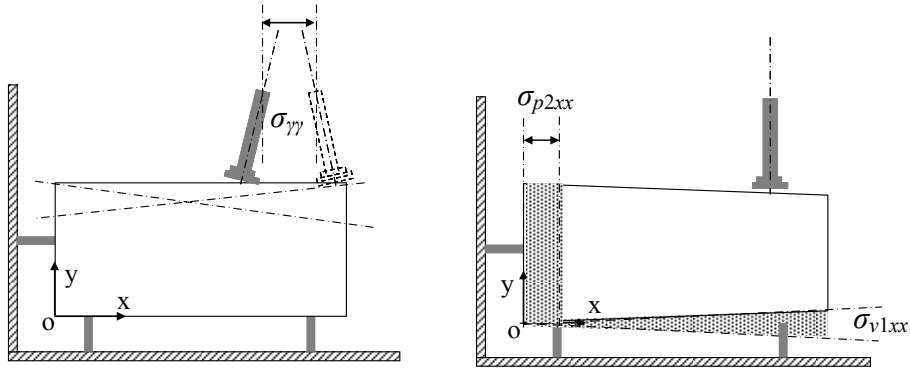


Figure 3.6 Variation Equivalence of Faulty Condition 5

$$\Sigma_{\mathbf{M}} = \begin{pmatrix} \sigma_{yyN} + f_{1x}^2 \sigma_{\gamma\gamma} & \sigma_{yyN} + f_{1x} f_{2x} \sigma_{\gamma\gamma} & \sigma_{xy} - f_{1x} f_{3y} \sigma_{\gamma\gamma} \\ \sigma_{yyN} + f_{1x} f_{2x} \sigma_{\gamma\gamma} & \sigma_{yyN} + f_{2x}^2 \sigma_{\gamma\gamma} & \sigma_{xy} - f_{2x} f_{3y} \sigma_{\gamma\gamma} \\ \sigma_{xy} - f_{1x} f_{3y} \sigma_{\gamma\gamma} & \sigma_{xy} - f_{2x} f_{3y} \sigma_{\gamma\gamma} & \sigma_{xx} + f_{3y}^2 \sigma_{\gamma\gamma} \end{pmatrix}, \quad (3.7a)$$

$$\Sigma_{\mathbf{D}} = \begin{pmatrix} \sigma_{p1yyN} + f_{1x}^2 \sigma_{v1xx} & \sigma_{p1yy} + f_{1x} f_{2x} \sigma_{v1xx} & \sigma_{\varepsilon\varepsilon} \\ \sigma_{p1yyN} + f_{1x} f_{2x} \sigma_{v1xx} & \sigma_{p1yy} + f_{2x}^2 \sigma_{v1xx} & \sigma_{\varepsilon\varepsilon} \\ \sigma_{\varepsilon\varepsilon} & \sigma_{\varepsilon\varepsilon} & \sigma_{p2xx} + f_{3y}^2 \sigma_{v2yy} \end{pmatrix}. \quad (3.7b)$$

- *Faulty condition 6: there are large variations of position in both x and y directions.*

This case has variations of displacements in two directions, which is explained by Fig.

3.7, Eqn. (3.8a) and (3.8b).

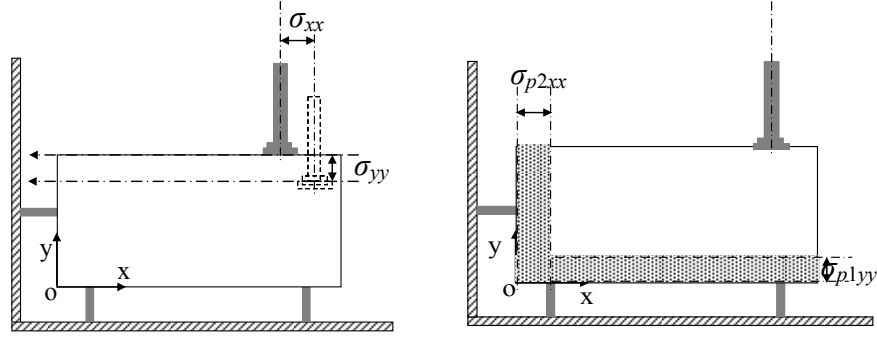


Figure 3.7 Variation Equivalence of Faulty Condition 6

$$\Sigma_{\mathbf{M}} = \begin{pmatrix} \sigma_{yy} + f_{1x}^2 \sigma_{\gamma\gamma N} & \sigma_{yy} + f_{1x} f_{2x} \sigma_{\gamma\gamma N} & \sigma_{xy} - f_{1x} f_{3y} \sigma_{\gamma\gamma N} \\ \sigma_{yy} + f_{1x} f_{2x} \sigma_{\gamma\gamma N} & \sigma_{yy} + f_{2x}^2 \sigma_{\gamma\gamma N} & \sigma_{xy} - f_{2x} f_{3y} \sigma_{\gamma\gamma N} \\ \sigma_{xy} - f_{1x} f_{3y} \sigma_{\gamma\gamma N} & \sigma_{xy} - f_{2x} f_{3y} \sigma_{\gamma\gamma N} & \sigma_{xx} + f_{3y}^2 \sigma_{\gamma\gamma N} \end{pmatrix}, \quad (3.8a)$$

$$\Sigma_{\mathbf{D}} = \begin{pmatrix} \sigma_{p1yy} + f_{1x}^2 \sigma_{v1xxN} & \sigma_{p1yy} + f_{1x} f_{2x} \sigma_{v1xxN} & \sigma_{\epsilon\epsilon} \\ \sigma_{p1yy} + f_{1x} f_{2x} \sigma_{v1xxN} & \sigma_{p1yy} + f_{2x}^2 \sigma_{v1xxN} & \sigma_{\epsilon\epsilon} \\ \sigma_{\epsilon\epsilon} & \sigma_{\epsilon\epsilon} & \sigma_{p2xx} + f_{3y}^2 \sigma_{v2yyN} \end{pmatrix}. \quad (3.8b)$$

- *Faulty condition 7: all the positional and normal variations are large.* This will be the most general case, in which all fault will occur in the process. The Fig. 3.8 shows this case. The covariance matrices of EFE due to machine tool error and due to datum error are given by Eqn. (3.9a) and (3.9b).

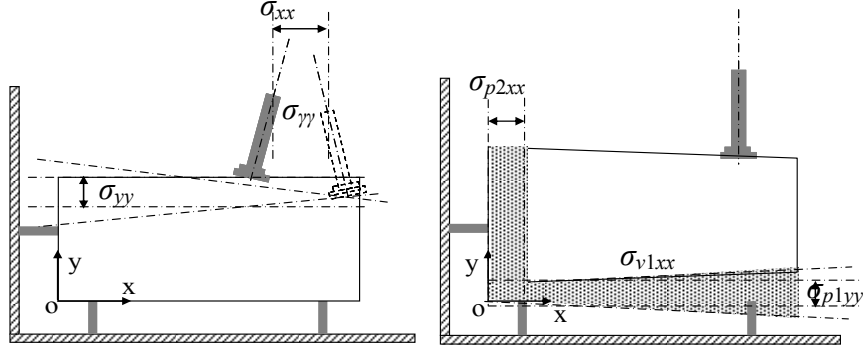


Figure 3.8 Variation Equivalence of Faulty Condition 7

$$\Sigma_{\mathbf{M}} = \begin{pmatrix} \sigma_{yy} + f_{1x}^2 \sigma_{\gamma\gamma} & \sigma_{yy} + f_{1x} f_{2x} \sigma_{\gamma\gamma} & \sigma_{xy} - f_{1x} f_{3y} \sigma_{\gamma\gamma} \\ \sigma_{yy} + f_{1x} f_{2x} \sigma_{\gamma\gamma} & \sigma_{yy} + f_{2x}^2 \sigma_{\gamma\gamma} & \sigma_{xy} - f_{2x} f_{3y} \sigma_{\gamma\gamma} \\ \sigma_{xy} - f_{1x} f_{3y} \sigma_{\gamma\gamma} & \sigma_{xy} - f_{2x} f_{3y} \sigma_{\gamma\gamma} & \sigma_{xx} + f_{3y}^2 \sigma_{\gamma\gamma} \end{pmatrix}, \quad (3.9a)$$

$$\Sigma_{\mathbf{D}} = \begin{pmatrix} \sigma_{p1yy} + f_{1x}^2 \sigma_{v1xx} & \sigma_{p1yy} + f_{1x} f_{2x} \sigma_{v1xx} & \sigma_{\varepsilon\varepsilon} \\ \sigma_{p1yy} + f_{1x} f_{2x} \sigma_{v1xx} & \sigma_{p1yy} + f_{2x}^2 \sigma_{v1xx} & \sigma_{\varepsilon\varepsilon} \\ \sigma_{\varepsilon\varepsilon} & \sigma_{\varepsilon\varepsilon} & \sigma_{p2xx} + f_{3y}^2 \sigma_{v2yy} \end{pmatrix}. \quad (3.9b)$$

### 3.2 Diagnosis and Root Cause Identification under Variation Equivalence

Process root cause diagnosis usually contains two steps, with mapping the product feature variation patterns to the library patterns as first step, followed by distinguishing variation sources that cause the identified product feature variation patterns. The second step is more challenging under variation equivalence. Although some research work (e.g., Jin and Zhou, 2006b) has mentioned this case, there is still not an efficient approach developed in the literature. In this Section, we develop a so called excitation-response path approach that is able to distinguish multiple variation sources under variation equivalence.

In this thesis, we will assume that there are only machine tool error and datum error in the machining process. To identify from which variation sources a product feature fault pattern is generated, it is equivalently to distinguish the variation sources between  $\Sigma_M$  and  $\Sigma_D$ . In  $\Sigma_M$  and  $\Sigma_D$ , we can see that given a specific fixture locator layout, the covariance structure will change according to changes of variation sources magnitudes. Therefore, in order to develop a variation sources identification approach, we can conduct some analysis of the covariance structures of  $\Sigma_M$  and  $\Sigma_D$  under different variation source magnitude settings. One way to represent the covariance structure is to use the eigenvectors of the covariance matrices. Denote  $\mathbf{a}_i(\Sigma_M)$  and  $\mathbf{a}_i(\Sigma_D)$  as  $i$ th eigenvectors of  $\Sigma_M$  and  $\Sigma_D$ . To analyze how  $\mathbf{a}_i(\Sigma_M)$  and  $\mathbf{a}_i(\Sigma_D)$  change as variation sources magnitudes change, we can compute the eigenvectors gestures under different variation sources values. Denote  $\mathbf{a}_{ref}$  as reference vector. By computing the angles between the eigenvectors and  $\mathbf{a}_{ref}$ , we can obtain the eigenvectors gestures information. Denote  $\psi_m, \psi_d$  as the angles set between  $\mathbf{a}_{ref}$  and  $\mathbf{a}_i(\Sigma_M), \mathbf{a}_i(\Sigma_D)$ , respectively; and  $\sigma_m, \sigma_d$  as the variation sources set for  $\mathbf{a}_i(\Sigma_M)$  and  $\mathbf{a}_i(\Sigma_D)$ . The points set of  $(\sigma_m, \psi_m), (\sigma_d, \psi_d)$  will form two curve of eigenvectors angles VS variation sources values, for which we call excitation-response path.

Given a fixture layout, the  $\Gamma$  matrix will be fixed. Furthermore,  $\text{Var}(\mathbf{y}_d) = \text{Var}(\mathbf{y}_m)$  under variation equivalence. We thus have  $\Sigma_M \approx \Sigma_D$ . If take faulty condition 6 for example, we will have  $\sigma_{yy} + f_{1x}^2 \sigma_{\gamma\gamma N} = \sigma_{p1yy} + f_{1x}^2 \sigma_{v1xxN}$ ,  $\sigma_{yy} + f_{2x}^2 \sigma_{\gamma\gamma N} = \sigma_{p1yy} + f_{2x}^2 \sigma_{v1xxN}$ , and  $\sigma_{xx} + f_{3y}^2 \sigma_{\gamma\gamma N} = \sigma_{p2xx} + f_{3y}^2 \sigma_{v2yyN}$ , respectively. If  $\sigma_{\gamma\gamma N} = \sigma_{v1xxN} = \sigma_{v2yyN}$ , we will

see that under the same value setting of variation sources, i.e.,  $\sigma_{yy} = \sigma_{p1yy}$ , and  $\sigma_{xx} = \sigma_{p2xx}$ , the  $\Psi_m$ , will be equal to  $\Psi_d$  at each point. In this situation, the curve of  $(\sigma_m, \Psi_m)$  and  $(\sigma_d, \Psi_d)$  overlap each other, which makes the two variation sources undistinguishable.

Therefore, to utilize the excitation-response path for variation sources identification, we must make some assumptions. First of all, the normal condition variation sources magnitudes are assumed to be different, e.g.,  $\sigma_{yyN} \neq \sigma_{p1yyN}$ . Besides, we assume that there is single product feature fault pattern for each product feature. The reason for first assumption has been aforementioned. It is also practical in that datum variation is usually larger than machine tool variation. This assumption will enable the curves of  $(\sigma_m, \Psi_m)$  and  $(\sigma_d, \Psi_d)$  to be different with a proper selected  $\mathbf{a}_{ref}$ . We do not consider multiple product feature variation patterns, because that our key issue for this topic is to distinguish multiple variation sources from the same product feature variation pattern. Thus the second assumption is also necessary.

Under these assumptions, we can conduct a sequential testing procedure to distinguish the variation sources. The root cause identification procedures will be:

- *Plot the excitation-response path for possible variation sources.* Here we assume that there are variations of machine tool error and datum error, corresponding to two excitation-response paths. If the two variation sources simultaneously contribute to the detected part feature variation pattern, this will result in a mixture excitation-response path. For the mixture path, we can assume weight coefficients for

both variation sources, i.e.,  $\Sigma_{mixed} = \lambda_M \Sigma_M + \lambda_D \Sigma_D$ , where  $\lambda_M + \lambda_D = 1$ . In this case, there will be totally three excitation-response paths in the plot.

- *Estimate two covariance matrices of process errors from two consecutive samples.*

The estimation  $\hat{\Sigma}_{i\ddot{u}} = S_{i\ddot{u}}$ , with  $S_{i\ddot{u}}$  denoting the sample covariance matrices,  $i = 1, 2$ , and  $\hat{\mathbf{u}} = (\mathbf{\Gamma}^T \mathbf{\Gamma})^{-1} \mathbf{\Gamma}^T \mathbf{y}$ .

- *Calculate the first eigenvector angles of the two sample covariance matrices.* By selecting a reference vector  $\mathbf{a}_{ref}$ , we can obtain two eigenvectors angles  $\psi_i$ ,  $i = 1, 2$ .

- *Estimate the variation sources values.* Take faulty condition 3 for instance,  $\hat{\sigma}_{iyy} = S_{i\ddot{u}}(1, 1) - f_{1x}^2 \sigma_{\gamma\gamma N}$ , and  $\hat{\sigma}_{p1yy} = S_{i\ddot{u}}(1, 1) - f_{1x}^2 \sigma_{v1xxN}$ ,  $i = 1, 2$ . The  $S_{i\ddot{u}}(1, 1)$  denote the element of the intersection between the first row and the first column in  $S_{i\ddot{u}}$ .

- *Compare the slope of the line that connects the two sample points with the slope of excitation-response path and distinguish the variation sources.* For example, if the two points  $(\hat{\sigma}_{1yy}, \psi_1)$  and  $(\hat{\sigma}_{2yy}, \psi_2)$  is close to the machine tool excitation-response path, and the slope of the line that connects the two points is similar two the slope on the excitation-response path, the variation sources will be identified as from machine tool error. It is vise versa for variation sources from datum error.

The rationale behind these procedures is that the eigenvectors of different samples covariance matrices will be not the same and they usually have a deviate range. However, in general, if the sample size is large enough, the sample eigenvectors gestures should be very similar to the population eigenvector (i.e, the eigenvector on the excitation-response path). The two samples are corresponding to two points on the excitation-response path

graph. Thus the slope of the line segment that connects the two points thus will be similar to the slope of the tangent at the population curve point. The Fig. 3.9a and 3.9b illustrates this rationale.

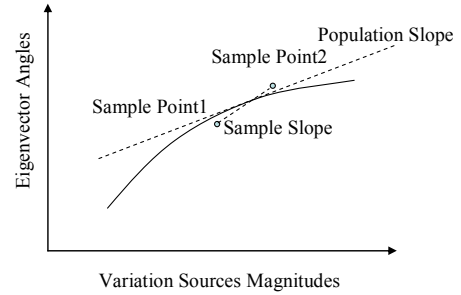
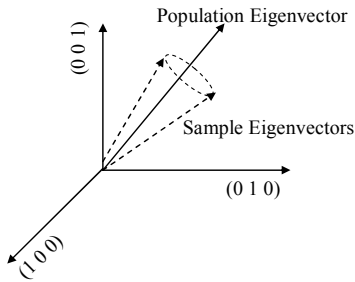


Figure 3.9a Eigenvectors Gestures      Figure 3.9b Sample Slope and Population Slope

### 3.3 Case Study

We will use a case study in this Section to verify this approach. In the case study, we use the block part shown in Fig. 3.1 as the example. The machining process is to mill the top surface.

#### 3.3.1 Illustration of the Root Cause Diagnosis Approach Using a Machining Process

The fixture locaters layout are specified as  $f_{1x} = 20, f_{2x} = 400, f_{3y} = 50$ . Suppose that the tolerance for translational error is  $\pm 0.55\text{mm}$ , and the tolerance for rotational error is  $\pm 0.0007\text{radian}$  ( $0.041\text{degree}$ ). The machining process is still to mill the top surface of a block part. There are two possible variation sources in the process, machine tool error and datum error. Normally, the machine tool angular error has smaller variation than the datum error. Thus, we suppose that  $\sigma_{xxN} = 0.2\text{mm}^2, \sigma_{yyN} = 0.2\text{mm}^2, \sigma_{xyN} = 0.000001\text{mm}^2,$

$\sigma_{\gamma\gamma N} = 0.0000008 \text{radian}^2$ ,  $\sigma_{v1xxN} = 0.000001$ ,  $\sigma_{p1yyN} = 0.3 \text{mm}^2$ ,  $\sigma_{v2yyN} = 0.000001$ ,  $\sigma_{p2xxN} = 0.3 \text{mm}^2$ , white noise  $\sigma_{\varepsilon\varepsilon} = 0.00000001 \text{mm}^2$ . We choose  $\mathbf{a}_{ref} = (0 \ 0 \ 1)^T$ . Suppose that product feature variation pattern of faulty condition 3 is detected, no mixture of two variation sources, and the true variation source is machine tool error with  $\sigma_{yy} = 0.36 \text{mm}^2$  (but actually we do not exactly know this value and which variation source occurs in the process). Here we collect two consecutive samples, with size  $n_1 = n_2 = 200$ . The first eigenvector angles of first and second samples are  $\psi_1 = 89.2007 \text{degree}$  and  $\psi_1 = 88.3643 \text{degree}$ . The estimated variation sources magnitudes are  $\hat{\sigma}_{1yy} = 0.3731 \text{mm}^2$  and  $\hat{\sigma}_{2yy} = 0.3458 \text{mm}^2$ , respectively. The results are summarized in Fig. 3.10.

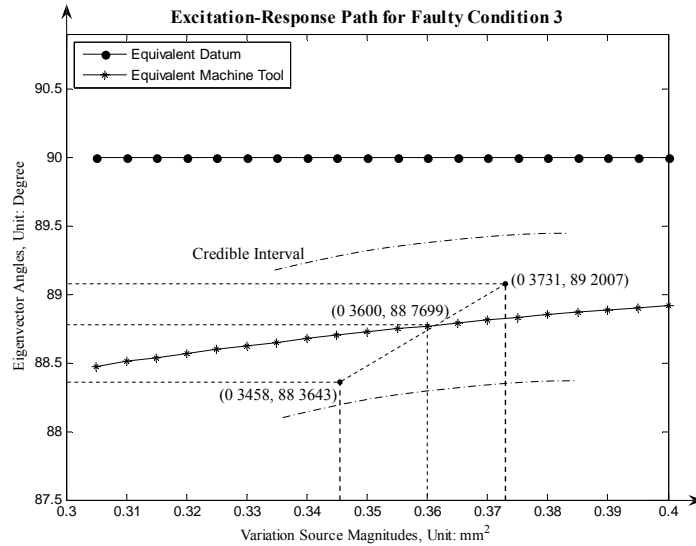


Figure 3.10 Excitation-Response Path of Case Study Result

In the excitation-response path plot, it is obvious that the sample data and its slope is more close to the population curve of machine tool. In light of this, we can determine that the variation source is from machine tool.

### 3.3.2 Remark on the Excitation-Response Path Approach

In the case study, we choose  $(0\ 0\ 1)^T$  as reference vector. The datum error curve is a horizontal line, which can be distinguished from machine tool error curve. However, if we choose  $(1\ 0\ 0)^T$  and  $(0\ 1\ 0)^T$  as reference vectors. The result will be different, and the root cause identification will be impossible. Because that the slopes of the two variation sources curve are the same, which makes the two curves parallel to each other. This is illustrated by Fig. 3.11 and Fig. 3.12. Therefore, for the excitation-response path approach, a reference vector that can distinguish the slopes of different variation sources curves is necessary.

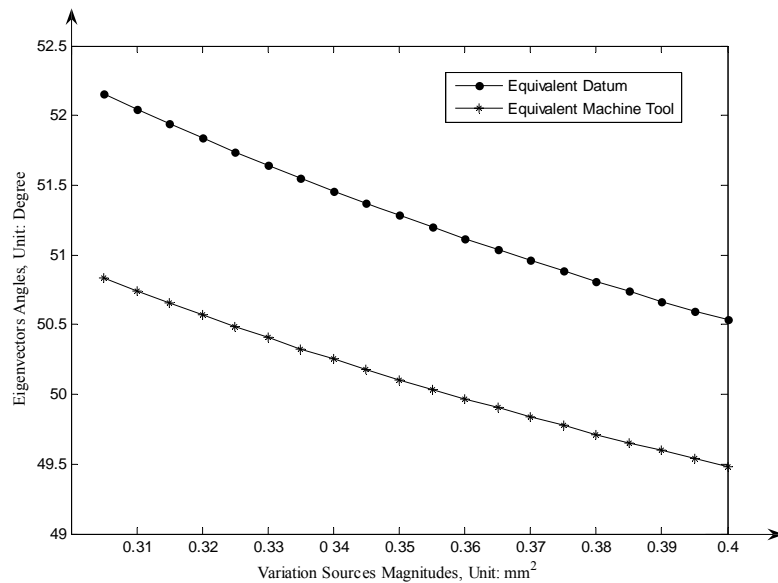


Figure 3.11 Excitation-Response Path Using Reference Vector  $(1\ 0\ 0)^T$

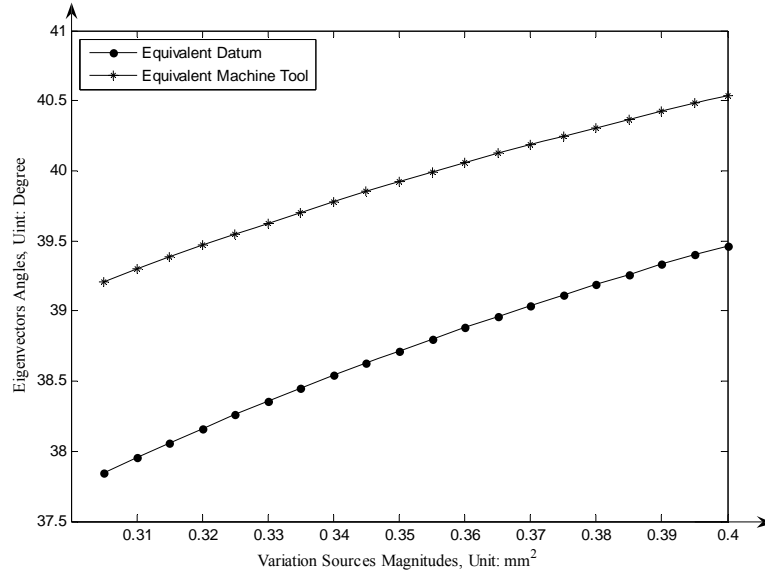


Figure 3.12 Excitation-Response Path Using Reference Vector  $(0\ 1\ 0)^T$

### 3.4 Chapter Summary

In this Chapter, the variation equivalence concept is presented and the equivalent variation patterns in machining process are explored. Based on the variation equivalence concept, we explore the possible product feature equivalent variation patterns among different variation sources, and construct the equivalent variation pattern library. By utilizing the library covariance structures and conducting some excitation-response path analysis, we find that different variation sources can be distinguished under variation equivalence. The case study well verifies this approach.

However, there is still limitation with regarding to this approach. For each faulty condition, a proper reference vector should be carefully selected. Otherwise, the root cause identification may fail if there is not a reference vector that can significantly

distinguish the slopes of different variation sources' excitation-response paths. For faulty condition 4 to faulty condition 7, each variation source has more than one variation elements. In this case, the excitation-response paths will not be a curve, but a surface, or even a volume. This will makes the visualized testing procedure more challenge, especially for 3-D cases.

## Chapter 4

### Conclusions and Future Work

#### 4.1 Conclusions

Manufacturing process design and control relies not only on an efficient process variation modeling, but also on many other variation reduction strategies. For early manufacturing process design stage, the efficiency of the design strategy usually relies on the dimensionality of the design space. For a good process control strategy, a method for efficiently diagnosing different variation sources is a must. The work in this thesis aims to develop efficient process design and process control strategies based on improving the understanding of error equivalence and variation phenomena, that is, different types of process errors and variation can result in the identical product feature deviation and variation. The implication of error equivalence mechanism can greatly impact the early stage design and quality control in manufacturing processes. The major contributions of this thesis are summarized as follows:

- *Process design and optimization based on error equivalence concept.* Due to the fact that different error sources can generate the same product feature deviation pattern, we can modeling the process variation propagation based on one error, i.e., the equivalent error or based error. An error equivalence based process tolerance stackup

model can thus be developed, and tolerance allocation can be conducted under a specified spatial layout. Meanwhile, embedding error equivalence into computer experiment design can assist us to search global optimal tolerance allocation among all the possible process tolerance design. Introducing the error equivalence mechanism into the to the process design significantly reduces the design space and relieve us from the considerable symbolic computation load, which results in a cost-effective design strategies.

- *Process control: root cause identification of variation sources under variation equivalence.* The variation equivalence phenomena expose the traditional manufacturing process diagnosis to the challenge that different variation sources may result in identical product feature variation patterns. Through exploring the possible product feature equivalent variation patterns among multiple error sources, we can construct the equivalent covariance structure library. Meanwhile, an excitation-response path orientation approach is developed to improve the variation sources root cause identification. The simulation study results show that this approach enables multiple variation sources to be distinguishable under variation equivalence.

## 4.2 Future Work

This study aims to improve manufacturing process design and control by using error equivalence methodology. In addition to the results obtained in process tolerance design, optimization, and process root cause diagnosis of variation sources under

variation equivalence, we can further expand the diagnosis approach to the processes that contain random effects. Since in practical machining processes, large variation random effects may occur due to unknown factors. The mixing of random effects with variation equivalence will lead the root cause diagnosis to a more challenging situation.

Furthermore, the limitations of the excitation-response path approach drive us to improve the testing procedures for higher dimensions of variation sources cases.

## Cited References

Agapiou, J. S., Steinhilper, E., Gu, F., and Bandyopadhyay, P., 2003, "A Predictive Modeling Methodology for Part Quality from Machining Lines," *NAMRI/SME Transactions*, XXXI, pp. 629~636.

Agapiou, J. S., Steinhilper, E., Bandyopadhyay, P., and Xie, J., 2005, "A Predictive Modeling Methodology for Part Quality from Machining Lines," *2005 ASME Mechanical Engineering Congress and Exposition, IMECE2005-79352*.

Apley, D., and Shi, J., 1998, "Diagnosis of Multiple Fixture Faults in Panel Assembly," *ASME Transactions, Journal of Manufacturing Science and Engineering*, 120, pp. 793~801.

Apley, D., and Shi, J., 2001, "A Factor-Analysis Method for Diagnosing Variability in Multivariate Manufacturing Processes," *Technometrics*, 43, pp. 84~95.

Bakker, T. M. D., 2000, *Design Optimization with Kriging Models*, Delft University press, WBBM Report Series 47.

Bernardo, M. C., Buck, R., Liu, L., Nazaret, W. A., Sacks, J., and Welch, W. J., 1992, "Integrated Circuit Design Optimization Using a Sequential Strategy," *IEEE Transaction, Computer-Aided Design*, 11, pp. 361~372.

Bjørke, Ø., 1989, *Computer Aided Tolerancing*, 2<sup>nd</sup> Edition, ASME Press, New York.

Cai, W., Hu, S. J., and Yuan, J. X., 1997, "A Variational Method of Robust Fixture Configuration Design for 3-D Workpieces," *ASME Transactions, Journal of Manufacturing Science and Engineering*, 119, pp. 593~602.

Camelio, J., Hu, S. J., and Ceglarek, D., 2003, "Modeling Variation Propagation of Multi-Station Assembly Systems with Compliant Parts," *ASME Transactions, Journal of Mechanical Design*, 125, pp. 673~681.

Camelio, J., and Hu, S. J., 2004, "Multiple Fault Diagnosis for Sheet Metal Fixtures Using Designated Component Analysis," *ASME Transactions, Journal of Manufacturing Science and Engineering*, 126, pp. 91~97.

Carlson, J. S., and Söderberg, R., 2003, "Assembly Root Cause Analysis: A Way to Reduce Dimensional Variation in Assembled Products," *International Journal of Flexible Manufacturing Systems*, 15, pp. 113~150.

Ceglarek, D., and Shi, J., 1996, "Fixture Failure Diagnosis for Auto Body Assembly Using Pattern Recognition," *ASME Transactions, Journal of Engineering for Industry*, 118, pp. 55~65.

Ceglarek, D., Shi, J., and Wu, S. M., 1994, "A Knowledge-Based Diagnostic Approach for the Launch of the Auto-Body Assembly Process," *ASME Transactions, Journal of Engineering for Industry*, 116, pp. 491~499.

Chang, M., and Gossard, D. C., 1998, "Computational Method for Diagnosis of Variation-Related Assembly Problem," *International Journal of Production Research*, 36, pp. 2985~2995.

Chase, K. W., and Greenwood, W. H., 1988, "Design Issues in Mechanical Tolerance Analysis," *Manufacturing Review*, 1, pp. 50~59.

Choi, H. G. R., Park, M. H., and Salisbury, E., 2000, "Optimal Tolerance Allocation with Loss Function," *ASME Transactions, Journal of Manufacturing Science and Engineering*, 122, pp. 273~281.

Cressie, N., 1993, *Statistics for spatial data*, Wiley, New York.

Ding, Y., Ceglarek, D., and Shi, J., 2002, "Fault Diagnosis of Multistage Manufacturing Processes by Using State Space Approach," *ASME Transactions, Journal of Manufacturing Science and Engineering*, 124, pp. 313~322.

Ding, Y., Jin, J., Ceglarek, D., and Shi, J., 2005, "Process-oriented Tolerancing for Multi-station Assembly Systems," *IIE Transactions on Design and Manufacturing*, 37, pp. 493~508.

Djurdjanovic, D., and Ni, J., 2001, "Linear State Space Modeling of Dimensional Machining Errors," *NAMRI/SME*, XXIX, pp. 541~548.

Dong, C., Zhang, C., Liang, Z., and Wang, B., 2005, "Dimensional Variation Analysis and Synthesis for Composite Components and Assemblies," *ASME Transactions, Journal of Manufacturing Science and Engineering*, 127, pp. 635~646.

Gupta, A., Ding, Y., Xu, L., and Reinikainen, T., 2006, "Optimal Parameter Selection for Electronic Packaging using Sequential Computer Simulations," *ASME Transactions, Journal of Manufacturing Science and Engineering*, 128(3), pp. 705~715.

Hong, Y. S., and Chang, T. C., 2002, "A Comprehensive Review of Tolerancing Research," *International Journal of Production Research*, 30, pp. 2425~2459.

Hu, S. J., 1997, "Stream of Variation Theory for Automotive Body Assembly," *Annals of CIRP*, 46(1), pp. 1~6.

Hu, S. J., and Wu, S. M., 1992, "Identifying Root Cause of Variation in Automobile Body Assembly Using Principal Component Analysis," *Transactions of NAMRI*, XX, pp. 311~316.

Huang, Q., and Shi, J., 2003, "Simultaneous Tolerance Synthesis through Variation Propagation Modeling of Multistage Manufacturing Processes," *NAMRI/SME Transactions*, 31, pp. 515~522.

Huang, Q., Shi, J., and Yuan, J., 2003, "Part Dimensional Error and Its Propagation Modeling in Multi-Operational Machining Process," *ASME Transactions, Journal of Manufacturing Science and Engineering*, 125, pp. 255~262.

Huang, Q., and Shi, J., 2004, "Variation Transmission Analysis and Diagnosis of Multi-Operational Machining Processes," *IIE Transactions on Quality and Reliability*, 36, pp. 807~815.

Huang, Q., Zhou, S., and Shi, J., 2002, "Diagnosis of Multi-Operational Machining Processes through Process Analysis," *Robotics and Computer-Integrated Manufacturing*, 18, pp. 233~239.

Jeang, A., 1994, "Tolerancing Design: Choosing Optimal Tolerance Specifications in the Design of Machined Parts," *Quality and Reliability Engineering International*, 10, pp. 27~35.

Jin, J., and Shi, J., 1999, "State Space Modeling of Sheet Metal Assembly for Dimensional Control," *ASME Transactions, Journal of Manufacturing Science and Engineering*, 121, pp. 756~762.

Jin, N., Zhou, S., 2006a, "Data-Driven Variation Source Identification of Manufacturing Processes Based on Eigenspace Comparison," *Naval Research Logistics*, 53(5), pp. 383~396.

Jin, N., Zhou, S., 2006b, "Signature Construction and Matching for Fault Diagnosis in Manufacturing Processes through Fault Space Analysis," *IIE Transactions*, 38, pp. 341~354.

Johnson, R. A., and Wichern, D. W., 1998, *Applied Multivariate Statistical Analysis*, 4<sup>th</sup> Edition, Prentice-Hall, Upper Saddle River, New Jersey.

Journel, A. G., and Huijbregts, C. J., 1978, *Mining Geostatistics*, Academic Press London.

Lawless, J. F., Mackay, R. J., and Robinson, J. A., 1999, "Analysis of Variation Transmission in Manufacturing Process-Part I," *Journal of Quality Technology*, 31, pp. 131~142.

Li, B., and Rizos, C., 2005, "Utilizing Kriging to Generate a NLOS Error Correction Map for Network Based Mobile Positioning, Journal of Global Positioning Systems," *Journal of Global Positioning Systems*, 4, pp. 27~35.

Li, H., and Shin, Y. C., 2006, "A Comprehensive Dynamic End Milling Simulation Model," *ASME Transactions, Journal of Manufacturing Science and Engineering*, 128, pp. 86~95.

Li, Z., and Zhou, S., 2006, "Robust Method of Multiple Variation Sources Identification in Manufacturing Processes for Quality Improvement," *ASME Transactions, Journal of Manufacturing Science and Engineering*, 128, pp. 326~336.

Li, Z., Zhou, S., and Ding, Y., 2007, "Pattern Matching for Root Cause Identification of Manufacturing Processes with Consideration of General Structured Noise," *IIE Transactions on Quality and Reliability Engineering*, 39, pp. 251~263.

Mantripragada, R., and Whitney, D. E., 1999, "Modeling and Controlling Variation Propagation in Mechanical Assemblies using State Transition Models," *IEEE Transactions on Robotics and Automation*, 15, pp. 124~140.

Matheron, G., 1963, "Principles of geostatistics," *Economic Geology*, 58, pp. 1246~1266.

McCullagh, P., and Nelder, J., 1989, *Generalized Linear Models*, 2<sup>nd</sup> edition, Chapman and Hall.

Montgomery, D. C., 2005, *Introduction to Statistical Quality Control*, 5<sup>th</sup> edition, Wiley, New York.

Nagarwala, M. Y., Pulat, P. S., and Raman, S. R., 1994, "Process selection and tolerance allocation for minimum cost assembly," *Manufacturing Science and Engineering*, ASME Bound Volume PED- 68, pp. 47~55.

Ngoi, B. K. A., and Ong, C. T., 1998, "Product and Process Dimensioning and Tolerancing Techniques: A State-of-the-Art Review," *International Journal of Advanced Manufacturing Technology*, 14, pp. 910~917.

Ngoi, B. K. A., and Ong, C. T., 1993, "A Complete Tolerance Charting System," *International Journal of Production Research*, 31, pp. 453~469.

Ngoi, B. K. A., and Ong, J. M., 1999, "A Complete Tolerance Charting System in Assembly," *International Journal of Production Research*, 37, pp. 2477~2498.

Pinheiro, J. C., and Bates, D. M., 2000, *Mixed-Effects Models in S and S-PLUS*, Springer, New York.

Pramanik, N., Roy, U., Sudarsan, R., and Sriram, R. D., 2005, "A Generic Deviation-Based Approach for Synthesis of Tolerances," *IEEE Transactions on Automation Science and Engineering*, 2, pp. 358~368.

Rao, C. R., 1972, "Estimation of Variance and Covariance Components in Linear Models," *Journal of America Statistics Association*, 67, pp. 112~115.

Rao, C. R., and Kleffe, J., 1988, *Estimation of Variance Components and Applications*, Amsterdam, The Netherlands: North-Holland.

Rong, Q., Ceglarek, D., and Shi, J., 2000, "Dimensional Fault Diagnosis for Compliant Beam Structure Assemblies," *ASME Transactions, Journal of Manufacturing Science and Engineering*, 122, pp. 773~780.

Roy, U., Liu, C. R., and Woo, T. C., 1991, "Review of Dimensioning and Tolerancing: Representation and Processing," *Computer-Aided Design*, 23, pp. 466~483.

- Sacks, J., Welch, W. J., Mitchell, T. J., and Wynn, H. P., 1989, "Design and Analysis of Computer Experiments", *Statistical Science*, 4, pp. 409~435.
- Santner, T. J., Williams, B. J., and Notz, W. I., 2003, *Design and Analysis of Computer Experiments*, Springer Series in Statistics, Springer Verlag, Berlin.
- Shiu, B. W., Apley, D. W., Ceglarek, D., and Shi, J., 2003, "Tolerance Allocation for Compliant Beam Structure Assemblies," *IIE Transactions on Design and Manufacturing*, 35, pp. 329~342.
- Singh, P. K., Jain, P. K., and Jain, S. C., 2004, "A Genetic Algorithm-based Solution to Optimal Tolerance Synthesis of Mechanical Assemblies with Alternative Manufacturing Processes: Focus on Complex Tolerancing Problems," *International Journal of Production Research*, 42, pp. 5185~5215.
- Taguchi, G., 1989, *Quality Engineering in Production Systems*, McGraw-Hill, New York.
- Torczon, V. J., 1997, "On the Convergence of Pattern Search Algorithm," *SIAM, Journal on Optimization*, 7, pp. 1~25.
- Voelcker, H. B., 1998, "The Current State of Affairs in Dimensional Tolerancing," *Integrated Manufacturing Systems*, 9, pp. 205~217.
- Wade, O. R., 1967, *Tolerance Control in Design and Manufacturing*, Industry Press, New York.
- Wang, H., Huang, Q., and Katz, R., 2005, "Multi-Operational Machining Processes Modeling for Sequential Root Cause Identification and Measurement Reduction," *ASME Transactions, Journal of Manufacturing Science and Engineering*, 127, pp. 512~521.
- Wang, H., and Huang, Q., 2006, "Error Cancellation Modeling and Its Application in Machining Process Control," *IIE Transactions on Quality and Reliability*, 38, pp. 379~388.
- Wang, P., and Liang, M., 2005, "Simultaneously Solving Process Selection, Machining Parameter Optimization, and Tolerance Design Problems: A Bi-Criterion Approach," *ASME Transactions, Journal of Manufacturing Science and Engineering*, 127, pp. 533~544.

Welch, W. J., Buck, R. J., Sacks, J., and Wynn, H. P., 1992, "Screening, Predicting, and Computer Experiments," *Technometrics*, 34, pp. 15~25.

Williams, B. J., Santner, T. J., and Notz, W. I., 2000, "Sequential Design of Computer Experiments to Minimize Integrated Response Functions," *Statistica Sinica*, 10, pp. 1133~1152.

Xue, J., and Ji, P., 2005, "Tolerance Charting for Components with Both Angular and Square Shoulder Features," *IIE Transactions*, 37, pp. 815~825.

Ye, B., and Salustri, F. A., 2003, "Simultaneous Tolerance Synthesis for Manufacturing Quality," *Research in Engineering Design*, 14, pp. 98~106.

Zhang, C., and Wang, H., 1993, "Optimal Process Sequence Selection and Manufacturing Tolerance Allocation," *Journal of Design and Manufacturing*, 3, pp. 135~146.

Zhang, C., Wang, H., and Li, J., 1992, "Simultaneous Optimization of Design and Manufacturing Tolerances with Process/Machine Selection," *Annals of CIRP*, 41, pp. 569~572.

Zhang, G., 1997, "Simultaneous Tolerancing for Design and Manufacturing," *Advanced Tolerance Techniques*, edited by Zhang, H. C., John Wiley and Sons, Inc., pp. 207~231.

Zhou, S., Chen, Y., and Shi, J., 2004, "Root Cause Estimation and Statistical Testing for Quality Improvement of Multistage Manufacturing Processes," *IEEE Transactions on Automation Science and Engineering*, 1(1), pp. 73~83.

Zhou, S., Ding, Y., Chen, Y., and Shi, J., 2003, "Diagnosability Study of Multistage Manufacturing Processes Based on Linear Mixed-Effects Models," *Technometrics*, 45, pp. 312~325.

Zhou, S., Huang, Q., and Shi, J., 2003, "State Space Modeling of Dimensional Variation Propagation in Multistage Machining Process Using Differential Motion Vectors," *IEEE Transaction on Robotics and Automation*, 19, pp. 296~309.

## Appendices

Appendix A: Review of EFE and Derivation of  $\Delta d$

Wang *et al.*, 2006, gave the derivation of EFE

$$\mathbf{x}_2^* = \mathbf{K}_1(\mathbf{v}_I \ \mathbf{p}_I \ \mathbf{v}_{II} \ \mathbf{p}_{II} \ \mathbf{v}_{III} \ \mathbf{p}_{III})^T, \quad (\text{A1})$$

and

$$\mathbf{x}_1^* = \mathbf{K}_2 \mathbf{x}_1, \quad (\text{A2})$$

where

$$\mathbf{K}_1 = \begin{pmatrix} \mathbf{G}_1 & & \\ & \mathbf{G}_2 & \\ & & \mathbf{G}_3 \end{pmatrix}. \quad (\text{A3})$$

For the specific form of  $\mathbf{K}_1$  and  $\mathbf{K}_2$ , refer to Wang, Huang, Katz, 2006. If the coordinates are under GCS, the  $\mathbf{K}_1$  and  $\mathbf{K}_2$  matrices are changed accordingly in each operation. E.g., in our example, for operation 1

$$\mathbf{K}(1)_2 = \begin{pmatrix} 0 & 0 & -1 & -f(1)_{1y} & f(1)_{1x} & 0 \\ 0 & 0 & -1 & -f(1)_{2y} & f(1)_{2x} & 0 \\ 0 & 0 & -1 & -f(1)_{3y} & f(1)_{3x} & 0 \\ 0 & -1 & 0 & f(1)_{4z} & 0 & -f(1)_{4x} \\ 0 & -1 & 0 & f(1)_{5z} & 0 & -f(1)_{5x} \\ -1 & 0 & 0 & 0 & -f(1)_{6z} & f(1)_{6y} \end{pmatrix},$$

for operation 2

$$\mathbf{K}(2)_2 = \begin{pmatrix} 0 & -1 & 0 & f(2)_{1z} & 0 & -f(2)_{1x} \\ 0 & -1 & 0 & f(2)_{2z} & 0 & -f(2)_{2x} \\ 0 & -1 & 0 & f(2)_{3z} & 0 & -f(2)_{3x} \\ 0 & 0 & -1 & f(2)_{4y} & -f(2)_{4x} & 0 \\ 0 & 0 & -1 & f(2)_{5y} & -f(2)_{5x} & 0 \\ -1 & 0 & 0 & 0 & -f(1)_{6z} & f(1)_{6y} \end{pmatrix},$$

and

$$\mathbf{G}(2)_1 = -\begin{pmatrix} f(2)_{1x} & 0 & f(2)_{1z} & 0 & 1 & 0 \\ f(2)_{2x} & 0 & f(2)_{2z} & 0 & 1 & 0 \\ f(2)_{3x} & 0 & f(2)_{3z} & 0 & 1 & 0 \end{pmatrix}, \mathbf{G}(2)_2 = -\begin{pmatrix} f(2)_{4x} & f(2)_{4y} & 0 & 0 & 0 & 1 \\ f(2)_{5x} & f(2)_{5y} & 0 & 0 & 0 & 1 \end{pmatrix}, \mathbf{G}(2)_3 = -\begin{pmatrix} 0 & f(2)_{6y} & f(2)_{6z} & 1 & 0 & 0 \end{pmatrix}.$$

Appendix A: (Continued)

To calculate  $\mathbf{x}_2^*(2)$ , using the feature deviation from operation 1 with the nominal fixture layout (the nominal location of six locators in operation 2), we can derive the relation between  $\mathbf{x}_2^*(2)$  and  $\mathbf{u}(1)$  after linearization as:

$$\mathbf{x}_2^*(2) = \mathbf{K}\mathbf{u}(1), \quad (\text{A4})$$

where  $\mathbf{K}$  is the coefficient matrix. Then the EFE due to datum errors will be linearly add to operation 2 in the stackup model. The EFE due to datum errors calculated thus obtained are:

$$\mathbf{x}_2^*(2) = \begin{pmatrix} -0.951875\Delta f(1)_{4y} - 0.048125\Delta f(1)_{5y} + 0.255208\Delta f(1)_{1z} + 0.255208\Delta f(1)_{2z} - 0.510417\Delta f(1)_{3z} \\ -0.201875\Delta f(1)_{4y} - 0.798125\Delta f(1)_{5y} + 0.255208\Delta f(1)_{1z} + 0.255208\Delta f(1)_{2z} - 0.510417\Delta f(1)_{3z} \\ -0.576875\Delta f(1)_{4y} - 0.423125\Delta f(1)_{5y} + 0.046875\Delta f(1)_{1z} + 0.046875\Delta f(1)_{2z} - 0.09375\Delta f(1)_{3z} \\ \quad - 1.07476\Delta f(1)_{1z} - 0.108575\Delta f(1)_{2z} + 0.183333\Delta f(1)_{3z} \\ \quad - 1.07476\Delta f(1)_{1z} - 0.108575\Delta f(1)_{2z} + 0.183333\Delta f(1)_{3z} \\ \quad - \Delta f(1)_{6x} - 0.3275\Delta f(1)_{4y} + 0.3275\Delta f(1)_{5y} \end{pmatrix}.$$

## Appendix B: Prediction and Estimation of Kriging Model

After obtaining an experimental design  $\mathbf{S} = \{\mathbf{s}_1, \dots, \mathbf{s}_n\}$  with corresponding responses  $\mathbf{y}_s = \{y_1, \dots, y_n\}$ , the unknown parameters in the correlation function have to be estimated, which is obtained by MLE criteria, and boils down to the minimization of the function

$$\frac{1}{2}(n \ln \hat{\sigma}^2 + \ln \det \mathbf{R}), \quad (\text{B1})$$

where  $\mathbf{R}$  is correlation coefficient matrix, and

$$\mathbf{R} = \begin{pmatrix} R(\mathbf{s}_1, \mathbf{s}_1) & R(\mathbf{s}_1, \mathbf{s}_2) & \cdots & R(\mathbf{s}_1, \mathbf{s}_n) \\ R(\mathbf{s}_2, \mathbf{s}_1) & R(\mathbf{s}_2, \mathbf{s}_2) & \cdots & R(\mathbf{s}_2, \mathbf{s}_n) \\ \vdots & \vdots & \ddots & \vdots \\ R(\mathbf{s}_n, \mathbf{s}_1) & R(\mathbf{s}_n, \mathbf{s}_2) & \cdots & R(\mathbf{s}_n, \mathbf{s}_n) \end{pmatrix}.$$

Then, using generalized least square estimation (GLS), the unknown parameters  $\boldsymbol{\beta}$  and  $\sigma^2$  can be estimated as

$$\hat{\boldsymbol{\beta}} = (\mathbf{F}^T \mathbf{R}^{-1} \mathbf{F})^{-1} \mathbf{F}^T \mathbf{R}^{-1} \mathbf{y}_s, \quad (\text{B2})$$

and

$$\hat{\sigma}^2 = \frac{1}{n} (\mathbf{y}_s - \mathbf{F} \hat{\boldsymbol{\beta}})^T \mathbf{R}^{-1} (\mathbf{y}_s - \mathbf{F} \hat{\boldsymbol{\beta}}), \quad (\text{B3})$$

where  $\mathbf{F} = [\mathbf{f}(\mathbf{s}_1), \dots, \mathbf{f}(\mathbf{s}_n)]^T$  is the regression design matrix. As for these parameter estimations, the best linear unbiased predictor (BLUP) is:

$$\hat{y}(\mathbf{w}) = \mathbf{f}^T(\mathbf{w}) \hat{\boldsymbol{\beta}} + \mathbf{r}^T(\mathbf{w}) \mathbf{R}^{-1} (\mathbf{y}_s - \mathbf{F} \hat{\boldsymbol{\beta}}), \quad (\text{B4})$$

where  $\mathbf{r}^T = [R(\mathbf{s}_1, \mathbf{w}), \dots, R(\mathbf{s}_n, \mathbf{w})]^T$  is a column matrix of correlation between the stochastic processes at given experimental design sites and untried input site. The mean squared error (MSE) was given by Sacks *et al.*, 1989, as:

$$MSE(\hat{y}(\mathbf{w})) = \hat{\sigma}^2 \{1 - [\mathbf{f}^T(\mathbf{w}) \quad \mathbf{r}^T(\mathbf{w})] \begin{bmatrix} \mathbf{0} & \mathbf{F}^T \\ \mathbf{F} & \mathbf{R} \end{bmatrix}^{-1} \begin{bmatrix} \mathbf{f}^T(\mathbf{w}) \\ \mathbf{r}^T(\mathbf{w}) \end{bmatrix}\}. \quad (\text{B5})$$

## Appendix C: Derivation of the Equivalent Covariance Structures

The derivation of the equivalent covariance matrices are based on the error equivalence model in Wang *et al.*, 2005. For 3-D case, we can obtain the covariance matrices of EFE due to machine tool error and datum error as  $\mathbf{K}_2 \boldsymbol{\Sigma}_{x_1} \mathbf{K}_2^T$  and  $\mathbf{K}_1 \boldsymbol{\Sigma}_{x_2} \mathbf{K}_1^T$ , where  $\boldsymbol{\Sigma}_{x_1}$  and  $\boldsymbol{\Sigma}_{x_2}$  are the covariance matrices of individual machine tool error and datum error. The details of  $\mathbf{K}_1$  and  $\mathbf{K}_2$  matrices are presented in Appendix A. For 2-D case, the derivation can be based on 3-D derivation. We can suppose there is no error for primary datum surface in 3-D case, which will result in 2-D case  $\mathbf{K}_1$ , i.e.,

$$\mathbf{x}_2 = [0 \ 0 \ 0 \ 0 \ 0 \ 0 \ 0 \ v_{IIx} \ v_{IIy} \ 0 \ p_{IIx} \ p_{IIy} \ 0 \ v_{IIIx} \ v_{IIIy} \ 0 \ p_{IIIx} \ p_{IIIy} \ 0]^T. \quad (C1)$$

Plug Eqn. (C1) into Eqn. (2.1), we can obtain the 2-D case product feature deviation  $\mathbf{y}_j(k)$ , i.e.,  $[0 \ 0 \ 0 \ -p_{IIy} - v_{IIy} f_{1x} \ -p_{IIy} - v_{IIy} f_{2x} \ -p_{IIIx} - v_{IIIx} f_{3y}]^T$ . Extracting the coefficients of individual datum error, we thus obtain  $\mathbf{K}_1$  as

$$\mathbf{K}_1 = \begin{pmatrix} -f_{1x} & 0 & 0 & -1 & 0 & 0 & 0 & 0 \\ -f_{2x} & 0 & 0 & -1 & 0 & 0 & 0 & 0 \\ 0 & 0 & 0 & 0 & 0 & -f_{3y} & -1 & 0 \end{pmatrix}. \quad (C2)$$

By setting 0 to the elements that are relevant to  $z$  direction, covariate terms between normal vector and position, or primary datum surface in 3-D case  $\boldsymbol{\Sigma}_{x_2}$ , e.g.,  $\sigma_{p_{IIz}} = 0$ ,  $\sigma_{v_{IIx} p_{IIy}} = 0$ , or  $\sigma_{v_{IIx}} = 0$ , we can obtain Eqn. (3.2b). For equivalent covariance structure of machine tool error, the derivation is similar, and

$$\mathbf{K}_2 = \begin{pmatrix} 0 & -1 & -f_{1x} \\ 0 & -1 & -f_{2x} \\ -1 & 0 & -f_{3y} \end{pmatrix}. \quad (C3)$$

### About the Author

Shaoqiang Chen received a Bachelor's Degree in Mechanical Engineering from Shanghai Jiao Tong University, Shanghai, China in 2004. He is currently a MSIE student in the Department of Industrial and Management Systems Engineering at the University of South Florida, Tampa, Florida, USA.

While in the MSIE program at the University of South Florida, Shaoqiang Chen focused on the research of manufacturing process design and process control. Currently, he is a member of IIE and a member of INFORMS-USF student chapter.